EUROPEAN ORGANIZATION FOR NUCLEAR RESEARCH (CERN)

CERN-EP-2026-132
2026/11/13

CMS-EXO-24-016

Search for long-lived particles decaying into muons in proton-proton collisions at $\sqrt{s} = 13.6\,\text{TeV}$ using data scouting

The CMS Collaboration*

arXiv:2606.25840v3 [hep-ex] 10 Nov 2026

Abstract

A search for long-lived particles decaying into muons is performed using proton-proton collisions at $\sqrt{s} = 13.6\,\text{TeV}$, collected by the CMS experiment at the LHC in 2022 and 2023, corresponding to an integrated luminosity of $62.4\,\text{fb}^{-1}$. The data were collected using dedicated dimuon triggers with low transverse momentum thresholds, recorded with a high-rate data scouting trigger stream. This data stream retains a reduced amount of information at the high-level trigger, to explore otherwise inaccessible phase space at low multimuon invariant mass and nonzero displacement from the primary interaction vertex. No significant excess of events above the standard model prediction is found. Upper limits on branching fractions at 95% confidence level are set for a wide range of mass and lifetime hypotheses in several beyond the standard model frameworks, where the Higgs boson decays into long-lived dark photons or into dark partons that produce showers containing long-lived particles, or where a long-lived scalar resonance is produced from the decay of a b hadron. The resulting constraints improve and extend existing ones in large regions of the parameter space.

Published in the Journal of High Energy Physics as doi:10.1007/JHEP11(2026)004.

© 2026 CERN for the benefit of the CMS Collaboration. CC-BY-4.0 license

*See Appendix A for the list of collaboration members

1 Introduction

The origin of dark matter remains one of the outstanding puzzles in particle physics and cosmology, in spite of the cosmological evidence of its existence [1–4]. Dark matter is expected to interact very weakly, if at all, with standard model (SM) particles, except via gravity. This introduces the possibility of a hidden (dark) sector of matter [5–7]. Particles in the dark sector would interact with the SM particles only via weakly interacting mediators.

One dark-matter scenario, referred to as the hidden Abelian Higgs model (HAHM), involves a spontaneously broken dark $U(1)_{\mathrm{D}}$ gauge symmetry, mediated by a dark photon, $\mathrm{Z_D}$ [6]. In this scenario, the only renormalizable interaction with SM particles occurs via the kinetic mixing of a dark photon with a hypercharge gauge boson. In addition, if a dark Higgs mechanism is responsible for the spontaneous breaking of the $U(1)_{\mathrm{D}}$ gauge symmetry, then the dark Higgs boson ($\mathrm{H_D}$) has a renormalizable coupling to the 125 GeV SM-like Higgs boson (H), resulting in mixing between the two physical scalar states. Thus, the hidden sector may interact with the SM sector either through the hypercharge portal via the kinetic mixing parameter ϵ, or through the Higgs portal via the Higgs mixing parameter κ. The dark photon $\mathrm{Z_D}$ may also mix with the SM photon (γ) and the Z boson through the hypercharge portal. If there are no hidden-sector states below the $\mathrm{Z_D}$ boson mass, the $\mathrm{Z_D}$ decays exclusively into SM particles, with a sizable branching fraction to leptons, where the coupling of the SM fermions to the $\mathrm{Z_D}$ boson is proportional to ϵ. The $\mathrm{Z_D}$ boson is expected to be long-lived if $\epsilon \lesssim 10^{-4}$, with a mean proper decay length $c\tau_0^{\mathrm{Z_D}} \gtrsim 1$ μm, proportional to ϵ^{-2}. In this regime, the decays $\mathrm{H} \to \mathrm{ZZ_D}$ and $\mathrm{H} \to \mathrm{Z_D Z_D}$ through the hypercharge portal have negligible branching fractions, hence the decays through the Higgs portal are expected to dominate. The diagrams in Fig. 1 illustrate the production of a pair of $\mathrm{Z_D}$ bosons in a Higgs boson decay.

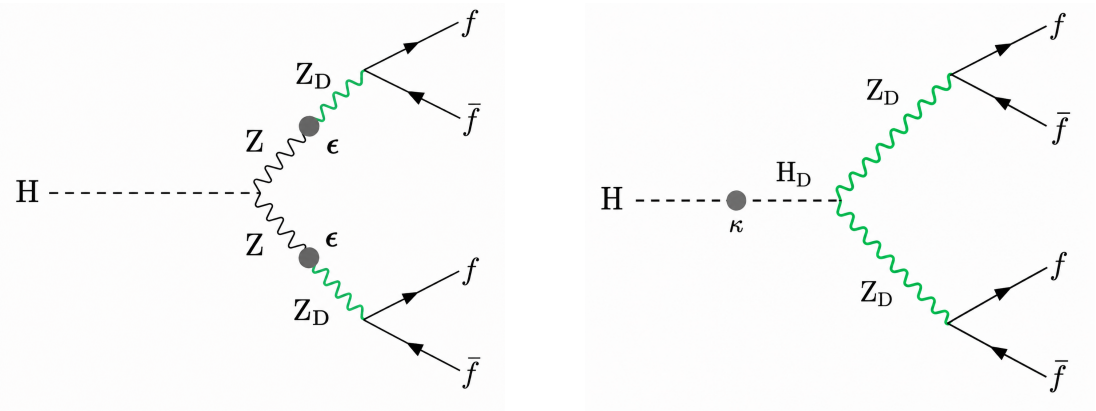

Figure 1: Diagrams illustrating an SM-like Higgs boson (H) decay to four fermions (f) via two intermediate dark photons, $\mathrm{Z_D}$ [6]: through the hypercharge portal (left) and the Higgs portal (right) via a dark Higgs boson ($\mathrm{H_D}$). The long-lived particles are highlighted in green.

In other hidden-sector models [8], a new, confining dark gauge group is introduced, which can produce events with multiple nonisolated dark particles, referred to as "dark showers", analogous to phenomena in the quantum chromodynamics sector of the SM. A spontaneously broken $U(1)$ gauge symmetry is involved, mediated by a dark photon $\mathrm{A'}$ that couples to the SM photon. The confining dark gauge group dynamically breaks the hidden-sector $SU(2) \otimes SU(2)$ flavor symmetry, resulting in the addition of a set of three dark pions ($\widetilde{\pi}_1$, $\widetilde{\pi}_2$, and $\widetilde{\pi}_3$) and a heavier dark meson, $\widetilde{\eta}$. In these models, the SM Higgs boson can decay into a pair of dark partons $\Psi\overline{\Psi}$, which then undergo showering and hadronization within the dark sector. Different scenarios are considered: a model where the dark photon $\mathrm{A'}$ is long-lived, referred

to as *Scenario A* [8], and a model where the dark pion $\widetilde{\pi}_3$ is long-lived instead, referred to as *Scenario B1* [8]. In both scenarios, it is assumed that the three dark pions $\widetilde{\pi}_1$, $\widetilde{\pi}_2$, and $\widetilde{\pi}_3$ have nearly degenerate masses $m_{\widetilde{\pi}}$ and arise from the decay of $\widetilde{\eta}$, $\widetilde{\eta} \to 3\widetilde{\pi}$, with the $\widetilde{\eta}$ meson mass $m_{\widetilde{\eta}} > 3m_{\widetilde{\pi}}$. On average, five dark mesons per event are produced. The dark pion $\widetilde{\pi}_3$ is assumed to decay, in turn, into a pair of dark photons A′, while $\widetilde{\pi}_1$ and $\widetilde{\pi}_2$ are assumed to be stable. Thus, Scenario A yields final states where multiple fermion pairs are produced in as many distinct vertices, each corresponding to the decay of a dark photon A′. Conversely, Scenario B1 yields final states where four fermions emerge from the same displaced vertex. Diagrams illustrating Scenarios A and B1 are shown in Fig. 2.

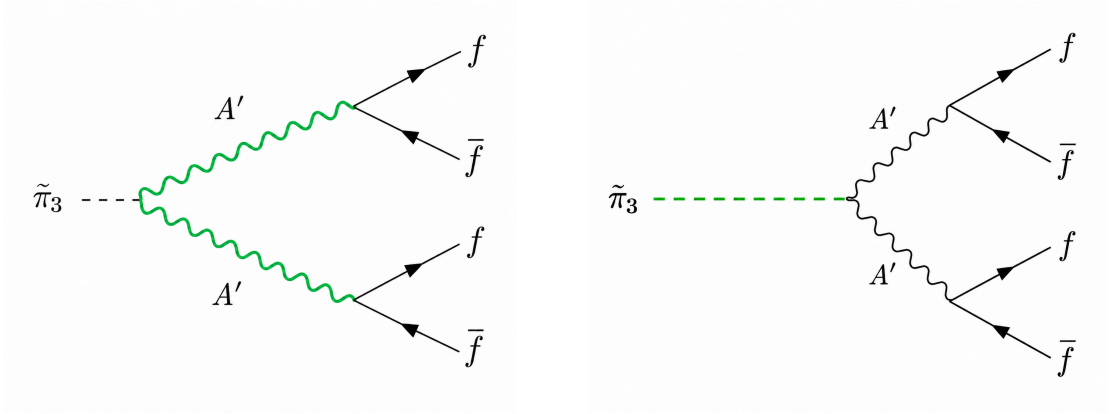

Figure 2: Diagrams illustrating two dark-shower scenarios [8], where a dark meson $\widetilde{\eta}$ is allowed to decay into dark pions ($\widetilde{\pi}_3$), which in turn decay into pairs of dark photons (A′). Scenario A (left) assumes prompt $\widetilde{\pi}_3$ decays into a pair of long-lived dark photons, A′, each decaying into fermions. Scenario B1 (right) assumes long-lived $\widetilde{\pi}_3$ decays into a pair of promptly decaying dark photons (A′). The long-lived particles are highlighted in green.

Constraints have been placed on visible dark-photon decays by beam dump [9], fixed-target [10], e^+e^- collider [11], and rare-decay experiments [12], as well as by the LHCb [13–15], ATLAS [16–18], and CMS [19–23] experiments at the CERN LHC.

Other scenarios of physics beyond the SM (BSM) are also considered that may produce a long-lived, low-mass resonance decaying into a muon pair. In one of the minimal extensions of the SM a singlet scalar field ϕ is added, which mixes with the Higgs boson with a mixing angle θ and thereby couples to all SM fermions [24, 25]. The ϕ boson is expected to be long-lived under the hypothesis of weak couplings to SM fermions, corresponding to $\theta \lesssim 10^{-3}$. Such a scalar resonance can be produced in decays of b hadrons, $h_b \to \phi X$. This process is depicted in Fig. 3. Constraints on this model have been previously set by the CHARM [26], LHCb [27, 28], and CMS [20] experiments.

This paper presents a search for narrow, long-lived multimuon resonances, based on data collected with the CMS experiment in proton-proton (pp) collisions at $\sqrt{s} = 13.6$ TeV in 2022 and 2023. A dedicated dimuon trigger stream (*scouting* [29]) with low transverse momentum (p_T) thresholds, recorded at high rate by retaining a reduced amount of information at the high-level trigger (HLT) is used. The rate of scouting triggers is higher than that of the standard triggers owing to less stringent requirements that enable multimuon resonance searches across mass and lifetime ranges that are otherwise inaccessible. The selected data correspond to a total integrated luminosity of 62.4 fb^{-1} (34.6 and 27.8 fb^{-1} collected in 2022 and 2023, respectively).

The search targets narrow, low-mass, long-lived resonances decaying into pairs of oppositely

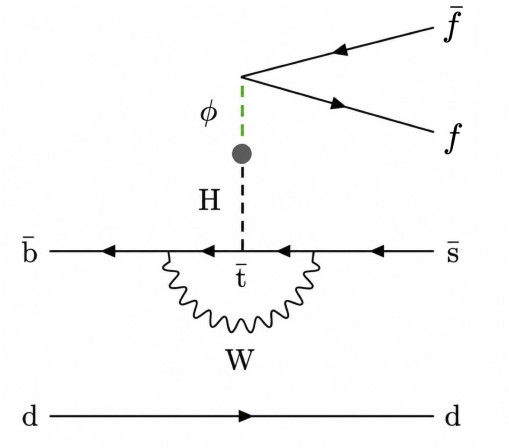

Figure 3: Diagram illustrating the production of a scalar resonance ϕ in a b hadron decay, through the mixing with an SM-like Higgs boson (H). The long-lived particle ϕ is highlighted in green.

charged muons, where the lifetime of the long-lived particle is such that the transverse displacement (l_{xy}) of its decay vertex is within roughly 70 cm of the primary vertex (PV) of the hard scattering, i.e., sufficiently within the volume of the tracker detector to ensure accurate measurements. The signal is expected to appear as a narrow peak on top of a smooth multimuon invariant mass distribution, with a resonance width that is assumed to be smaller than the experimental mass resolution. The search is performed by looking for localized excesses in the multimuon invariant mass spectrum across different ranges of l_{xy}. We probe, for the first time in CMS, multimuon final states with large displacements and masses below 10 GeV, which have not been explored so far owing to the limitations of the standard trigger streams and of the dimuon scouting triggers used by CMS before 2022. In particular, the improvements in the dimuon scouting triggers allow for the reconstruction of displaced muon pairs beyond 11 cm in l_{xy}, which was a limitation of the analysis presented in Ref. [20], where data collected with the scouting triggers available in 2017 and 2018 were used. Moreover, the extended event content available in the scouting data collected since 2022 [29] is exploited to further improve the sensitivity of the search.

This paper is organized as follows. The CMS detector, and the data sets and triggers used in the analysis are described in Sections 2 and 3, respectively. The signal Monte Carlo (MC) samples for each interpretation are presented in Section 4. The event selection and categorization strategies are discussed in Section 5, while Section 6 outlines the modeling of the signal and the background. Finally, results are presented in Section 7, and the paper is summarized in Section 8. Tabulated results are available in the HEPData record for this analysis [30].

2 The CMS detector

The central feature of the CMS apparatus is a superconducting solenoid of 6 m internal diameter providing a magnetic field of 3.8 T. Within the solenoid volume are a silicon pixel and strip tracker, a lead tungstate crystal electromagnetic calorimeter, and a brass and scintillator hadron calorimeter, each composed of a barrel and two endcap sections. Forward calorimeters extend the pseudorapidity (η) coverage provided by the barrel and endcap detectors. Muons are reconstructed using gas-ionization detectors interleaved with the layers of the steel flux-return yoke outside the solenoid. A global "particle-flow" (PF) algorithm [31] aims to reconstruct all

individual particles in an event, combining information provided by the all-silicon tracker and by the calorimeters with data from the gas-ionization muon detectors. The pixel tracker consists of four concentric barrel layers at radii of 2.9, 6.8, 10.9, and 16.0 cm, and three disks on each end at distances of 29.1, 39.6, and 51.6 cm from the center of the detector [32]. The region between 20 and 116 cm is occupied by the silicon strip tracker. Four barrel layers, supplemented by three disk in the endcaps, compose the tracker inner barrel and disks, which extends the radius up to 55 cm. Beyond this range, the tracker outer barrel and the tracker endcaps are situated, adding six layers and nine additional disks at each end. A more detailed description of the CMS detector, together with a definition of the coordinate system used and the relevant kinematic variables, can be found in Refs. [33, 34].

A two-level trigger system is used to select events of potential physics interest. The first level of the CMS trigger system (L1) [35], composed of custom hardware processors, uses information from the calorimeters and muon detectors to select events of interest in a fixed time interval of about 4 μs. The HLT processor farm further decreases the event rate from around 100 kHz to a few kHz, before data storage. A more detailed description of the CMS trigger system can be found in Refs. [36, 37].

In addition to the standard HLT selection streams, a dedicated set of triggers exists that allows the exploration of additional phase space. This approach is referred to as *data scouting* [29]. The scouting trigger algorithms used in this search select events containing muon pairs with a dimuon invariant mass greater than the muon mass ($m_{\mu\mu} \gtrsim 2m_{\mu}$) at a rate of a few kHz. In order to allow the large rate within an acceptable bandwidth, the event size is reduced by up to a factor of 1000 by only retaining limited information, as reconstructed at the HLT.

3 Data sets and triggers

The standard trigger streams typically select events containing at least one particle (e.g., a lepton) or jet with large p_{T}. Thus, such triggers are not necessarily ideal in a generic search for light, narrow resonances decaying into two muons with $p_{\mathrm{T}} \lesssim 10\,\mathrm{GeV}$. Muons are reconstructed at the HLT by combining the information from the tracker and the muon detectors. The retained limited information includes their four-momenta, the number of hits left in the tracker and in the muon detectors, and detailed information on the muon tracks. These muon tracks are used in pairs to form dimuon vertices, considering all possible pairs. In the following, these vertices are called secondary vertices (SVs), and they may be either displaced from the PV or not. Candidate pp interaction vertices are formed using tracks reconstructed from hits only in the pixel detector, and the candidate vertex with the largest value of summed track p_{T}^2 is taken to be the PV of the pp interaction. Events in the scouting data sets contain information on the normalized χ^2 of all reconstructed vertices, together with their position with respect to the nominal interaction point.

Between 2018 and 2022, the CMS muon scouting triggers [38] were updated, broadening the accessible phase space and increasing the amount of information retained for each event. The main improvement arises from the removal of the pixel hit multiplicity requirement, which previously prevented any muon with <2 pixel hits from being accepted by the scouting triggers. As a result, the muons with $l_{\mathrm{xy}} > 11\,\mathrm{cm}$ are now accessible for the first time in a search using scouting data. Additionally, more detailed information on tracks and PF candidates is retained and used to improve the background rejection, as described in Section 5.1.

Events are preselected at the L1 trigger with at least two muons passing requirements on the p_{T}, η and charge of each muon and on their angular separation, defined as $\Delta R(\mu_1, \mu_2) =$

$\sqrt{[\Delta\phi(\mu_1,\mu_2)]^2 + [\Delta\eta(\mu_1,\mu_2)]^2}$, where ϕ is the azimuthal angle and μ_1 (μ_2) is the leading (subleading) muon.

In 2022, events were required to pass at least one of three criteria:

- the presence of at least two opposite-sign (OS) L1 muons with $p_{\mathrm{T}}^{\mu} > 4\,\mathrm{GeV}$ and $\Delta R(\mu_1,\mu_2) < 1.2$;
- the presence of at least two OS L1 muons with $p_{\mathrm{T}}^{\mu} > 4.5\,\mathrm{GeV}$ and $|\eta^{\mu}| < 2.0$; or
- the presence of at least two L1 muons with $p_{\mathrm{T}}^{\mu_1} > 15\,\mathrm{GeV}$ and $p_{\mathrm{T}}^{\mu_2} > 7\,\mathrm{GeV}$.

In 2023, two additional L1 triggers were added, requiring:

- the presence of at least two OS L1 muons with $|\eta^{\mu}| < 1.4$ and $\Delta R(\mu_1,\mu_2) < 1.4$; or
- the presence of at least two L1 muons with $p_{\mathrm{T}}^{\mu} > 8\,\mathrm{GeV}$.

The measurement of the muon momentum at the L1 trigger relies only on the information from the muon detectors. After the L1 trigger preselections, only events containing two OS muons with $p_{\mathrm{T}}^{\mu} > 3\,\mathrm{GeV}$ and $|\eta^{\mu}| < 2.4$ are retained at the HLT, where the inner tracker information improves the muon p_{T} measurement and spatial resolution.

The efficiency of the scouting triggers is measured in data, as a function of the dimuon l_{xy} and of the minimum p_{T}^{μ} of the pair, using events with at least two muons selected with independent, orthogonal triggers based on calorimeter energy deposits. The measured efficiency and its uncertainty are accounted for in the normalization of simulated events, as discussed in Section 4.

Because only a reduced amount of information is available in the scouting data, no additional calibration is performed for the muons used in this search. The resulting dimuon mass resolution was measured to differ by less than 1% from that obtained using muons that undergo the full offline reconstruction [29], which has a negligible effect on the results presented in this paper.

4 Monte Carlo simulation

The SM background is estimated directly from data in the dimuon ($m_{\mu\mu}$) or four-muon ($m_{4\mu}$) invariant mass spectrum, parameterized by smooth analytical functions. Thus, the search does not rely on MC simulation in order to estimate the background.

On the other hand, MC simulations of BSM signals are used to interpret the results of the search. In particular, a model of Higgs boson production via the dominant mode of gluon-gluon fusion is simulated, with $\mathrm{H} \to \mathrm{Z_D Z_D}$, where $\mathrm{Z_D}$ is a long-lived resonance and at least one $\mathrm{Z_D}$ decays into a pair of OS muons. The phenomenology of this model is defined by four parameters:

- the kinetic mixing ϵ;
- the mass of the dark photon, $m_{\mathrm{Z_D}}$;
- the Higgs portal coupling, κ; and
- the mass of the dark Higgs boson, $m_{\mathrm{H_D}}$.

In the simulation used in this search, $m_{\mathrm{H_D}}$ and κ are fixed to 400 GeV and 0.01, respectively, in a regime where $\mathrm{H} \to \mathrm{H_D H_D}$ decays are kinematically forbidden. Instead, the Higgs boson is set to always decay into a pair of $\mathrm{Z_D}$ bosons, which in turn decay into SM fermions with branching fractions that depend on their mass [6]. The branching fraction for $\mathrm{Z_D}$ decays into muon

pairs varies from about 50% at a mass of 0.5 GeV to about 9% at a mass of 50 GeV. The lifetime of the Z_D boson for a given mass hypothesis is determined by ϵ. In this paper, dark photons are simulated with $c\tau_0^{Z_D} = 0.1$, 1, 10, and 100 cm, except for masses below 1 GeV, where only $c\tau_0^{Z_D} = 0.1$ and 1 cm scenarios are simulated to account for the variation in acceptance due to the large Lorentz boost of the particles, which results in longer decay lengths for low-mass resonances. A lifetime-based reweighting procedure is additionally employed to probe intermediate lifetime values. The production of dark photons is modeled at leading order (LO) with MADGRAPH5_aMC@NLO 2.9.9 [39]. While only the dominant gluon-gluon fusion production mechanism is considered for the generation, the Higgs boson production cross section is normalized to the most recent theoretical prediction for the sum of all production modes for the mass of Higgs boson $m_H = 125$ GeV at $\sqrt{s} = 13.6$ TeV, which is 59.8 pb [40, 41]. Other Higgs boson production mechanisms are not considered in the generation for simplicity, because they have negligible effects on the analysis acceptance. The decays of dark photons are simulated using PYTHIA 8.306 [42]. These samples are used to set upper limits on the branching fraction $\mathcal{B}(H \to Z_D Z_D)$, using values of $\mathcal{B}(Z_D \to \mu\mu)$ from the model of Ref. [6].

Dark-shower signal models are simulated at LO with PYTHIA 8.309 for selected mass combinations of Scenarios A and B1, considering two dark flavors and three dark colors. In these models, the SM Higgs boson is set to decay into a pair of dark partons $\Psi\overline{\Psi}$, which then undergo showering and hadronization within the dark sector. The Higgs boson production cross section is normalized to 59.8 pb [40, 41]. The mass scale is set by assuming $\tilde{\Lambda} = m_{\tilde{\eta}} = 4m_{\tilde{\pi}}$, where $\tilde{\Lambda}$ is the dark-sector confinement scale. The coupling of the dark photon to dark-sector quarks controls the isospin violation through the mixing angle θ. We consider $\sin\theta = 0.1$ to ensure that isospin breaking remains relatively small, resulting in the dark pions having nearly degenerate masses. The branching fraction $\mathcal{B}(\widetilde{\pi}_3 \to A'A')$ is set to unity. Samples are generated with different mass hypotheses for the $\widetilde{\pi}_3$ and the A' particles, and with mean proper decay lengths ranging from 0.01 to 100 cm for A' ($\widetilde{\pi}_3$) in Scenario A (B1). These samples are used to set upper limits on the branching fraction $\mathcal{B}(H \to \Psi\overline{\Psi})$.

For models where a long-lived scalar resonance ϕ arises from the decay of a b hadron, the production of b hadrons is initially generated at LO using PYTHIA 8.306, where the ϕ boson decays into a pair of OS muons with 100% probability. Subsequently, a fixed-order calculation at next-to-leading logarithmic (FONLL) precision in the strong coupling constant α_S is used to normalize the signal and to reweight the p_T spectrum of b hadrons. These samples are used to set upper limits on the branching fraction product $\mathcal{B}(h_b \to \phi X)\mathcal{B}(\phi \to \mu\mu)$.

The generators use the CP5 tune [43] and the NNPDF3.1 sets of parton distribution functions (PDFs) [44] at next-to-next-to-LO. The interactions of particles with the CMS detector are simulated using GEANT4 [45]. Simulated minimum bias events are superimposed on the hard pp interaction to describe the effect of additional inelastic interactions within the same or neighboring bunch crossings (pileup). The simulation is reweighted to match the distribution of the number of interactions per bunch crossing observed in data. All simulated events are reconstructed with the same algorithms used for data.

5 Event selection and categorization

5.1 Event selection

The events collected using the scouting triggers (Section 3) are further selected to contain at least one pair of OS muons associated with an SV that satisfies a number of quality criteria:

- $l_{xy} < 70\,\text{cm}$;
- x coordinate uncertainty $<0.05\,\text{cm}$;
- y coordinate uncertainty $<0.05\,\text{cm}$;
- z coordinate uncertainty $<0.10\,\text{cm}$;
- The SV fit χ^2 normalized to the number of degrees of freedom (dof) $\left(\chi^2/\text{dof}\right)_{\text{SV}} < 3$.

The $\left(\chi^2/\text{dof}\right)_{\text{track}}$ of each muon track is also required to be less than 3. Furthermore, any SV located within a tracker module is not considered in order to suppress the contribution from material interaction vertices, i.e., vertices from particles produced in the interactions with the detector material.

A large fraction of events contain only one OS muon pair and an associated SV. Among the events with more than one pair of OS muons, the pairs are ordered according to increasing $(\chi^2/\text{dof})_{\text{SV}}$ and only the first or the first two pairs are used in this search. If two muon pairs are reconstructed, the positions of the corresponding SVs may be spatially resolved or may overlap within uncertainties, thus appearing as a single four-muon (4μ) vertex. In this case, the average position of the two overlapping SVs is used as the position of the 4μ vertex, and the selections are adapted accordingly, as detailed in the following.

For decays of BSM particles into a single muon pair, we expect the transverse momentum of the dimuon system, $\vec{p}_{\text{T}}^{\,\mu\mu}$, to be collinear with the SV vector, which is defined as the vector $\overrightarrow{\text{SV}}$ connecting the PV to the SV. This does not apply to a muon pair where the two muons originate from different vertices and erroneously form a common SV because their trajectories accidentally cross. In order to suppress this background, we require both the azimuthal angle ($|\Delta\phi(\vec{p}_{\text{T}}^{\,\mu\mu}, \overrightarrow{\text{SV}})|$) and the three-dimensional angle between the two vectors to be less than $\pi/2$. This requirement is used in events with one or two resolved SVs. In events where four muons are selected from two SVs that overlap in space within uncertainties, hereafter referred to as *overlapping* SVs, we require the four-muon transverse momentum, $\vec{p}_{\text{T}}^{\,4\mu}$, to be collinear with the vector connecting the PV with the overlapping SVs. The same requirements on the azimuthal and three-dimensional angles are applied.

Similarly, the opening angle between two muons erroneously forming a common SV tends to be very large, independently of the boost of the dimuon system. Hence, in order to further reduce the background from events with an erroneous muon SV association, we also require both the azimuthal and three-dimensional angles between the muons to be <2.8. The main goal of such selections is to suppress background where SVs are formed by cosmic ray muons, muons from pileup interactions, and muons from back-to-back quantum chromodynamics dijet events or Drell–Yan events.

Muons from pileup vertices can overlap in the r-ϕ plane, despite being separated in r-z at their origin, and, as a consequence, they can be wrongly associated with a common SV. These muon pairs are characterized by a large $\Delta\eta(\mu_1, \mu_2)$ and a small $\Delta\phi(\mu_1, \mu_2)$. We exploit this feature to suppress this background contribution with the requirement $\log_{10}(|\Delta\eta_{\mu\mu}|/|\Delta\phi_{\mu\mu}|) < 1.25$. This requirement is not applied in cases with two selected muon pairs.

Additional background may arise from "prompt" (i.e., nondisplaced) muons. Muons from truly displaced vertices do not leave hits in the tracker layers between the interaction point and the SV. Therefore, this background can be suppressed by applying a selection on the number of hits associated with each muon between the PV and the SV, referred to as $N_{\text{excess}}^{\mu\mu}$:

- $N_{\text{excess}}^{\mu\mu} = 0$ for $l_{xy} < 11\,\text{cm}$;

- $N^{\mu\mu}_{\text{excess}} \leq 1$ for $l_{\text{xy}} \in [11, 16]$ cm;
- $N^{\mu\mu}_{\text{excess}} \leq 2$ for $l_{\text{xy}} \in [16, 70]$ cm.

The requirement is loosened for higher displacements, because at large values of l_{xy} it is more likely that random hits are wrongly associated with displaced muon tracks, and is fully relaxed in events where four muons from two overlapping SVs are selected.

In order to identify SVs of interest, the muon track transverse impact parameter, d_{xy}, is also used. Specifically, we select events based on the d_{xy} significance ($|d_{\text{xy}}|/\sigma_{d_{\text{xy}}}$) and the lifetime-scaled d_{xy} ($|d_{\text{xy}}|/(l_{\text{xy}} m_{\mu\mu}/p_{\text{T}}^{\mu\mu})$). The first expression normalizes d_{xy} to its measurement uncertainty ($\sigma_{d_{\text{xy}}}$), while the second normalizes d_{xy} to the lifetime corresponding to the observed SV transverse displacement. This allows the same selection requirements to be used for all lifetime hypotheses. We require each muon in dimuon events to satisfy:

- $|d_{\text{xy}}|/\sigma_{d_{\text{xy}}} > 2$;
- $|d_{\text{xy}}|/(l_{\text{xy}} m_{\mu\mu}/p_{\text{T}}^{\mu\mu}) > 0.1$.

In events with two muon pairs, where there are few background events, the selected muons are only required to have $|d_{\text{xy}}|/\sigma_{d_{\text{xy}}} > 2$.

Finally, in events with two muon pairs from spatially resolved SVs, the two dimuon invariant masses are further required to differ by less than 5% of their average.

The muon isolation is measured as the scalar p_{T} sum of the additional PF candidates within a cone of $\Delta R = \sqrt{(\Delta\eta)^2 + (\Delta\phi)^2} = 0.4$ around its direction, including corrections for the contributions from pileup. A muon is considered isolated if its isolation is less than 8 GeV and less than 20% of its p_{T}. These isolation criteria are only used to categorize events with only one selected muon pair, as described in Section 5.2.

5.2 Event categorization

Once the objects have been selected, three types of events are considered in the search:

- events with one muon pair;
- events with two muon pairs from two SVs whose positions are spatially resolved; and
- events with two muon pairs from two SVs whose positions overlap within uncertainties, consistent with a single 4μ vertex.

Because 4μ events are expected to provide sensitivity to a range of BSM scenarios and are depleted in background, we first select events with two muon pairs. If an event contains four muons from two resolved SVs, we then assign the event to the so-called *multivertex* category. If instead we identify four muons from two overlapping SVs, we assign the event to the *overlapping vertex* category. In both cases, the signal would appear as a narrow peak in the $m_{4\mu}$ spectrum.

If only one muon pair is found, the event is categorized as a dimuon event. For dimuon events, we first define two orthogonal regions in $|\Delta\phi(\vec{p}_{\text{T}}^{\,\mu\mu}, \overrightarrow{\text{SV}})|$, distinguishing *pointing* and *nonpointing* topologies, with $|\Delta\phi(\vec{p}_{\text{T}}^{\,\mu\mu}, \overrightarrow{\text{SV}})| < 0.02$ and $0.02 < |\Delta\phi(\vec{p}_{\text{T}}^{\,\mu\mu}, \overrightarrow{\text{SV}})| < \pi/2$, respectively.

Dimuon events in both the pointing and nonpointing categories are then further split according to l_{xy}, to maximize the sensitivity to different lifetime hypotheses. We define eight bins in l_{xy},

following the detector geometry:

- within the beam pipe: [0, 0.2] cm; [0.2, 1] cm; [1, 2.4] cm;
- between the beam pipe and the first pixel tracker layer: [2.4, 3.1] cm;
- between the first and second pixel tracker layers: [3.1, 7] cm;
- between the second and third pixel tracker layers: [7, 11] cm;
- between the third and fourth pixel tracker layers: [11, 16] cm; and
- outside the pixel tracker: [16, 70] cm.

The last two l_{xy} intervals probe phase space that was inaccessible to previous results using scouting data [20].

The overall signal acceptance times efficiency ($\mathcal{A}\varepsilon$) in the different l_{xy} categories is shown in Fig. 4 for representative HAHM dark photon mass hypotheses, $m_{Z_D} = 2, 5, 12$ and 20 GeV, as a function of the dark photon mean proper decay length, $c\tau_0^{Z_D}$. The signal $\mathcal{A}\varepsilon$ is defined as the fraction of events with at least one dark photon decaying into a muon pair, reconstructed as a single dimuon candidate within the specified displacement range. It is a luminosity-weighted average over the 2022 and 2023 data-taking periods. The increase in acceptance resulting from the newly accessible $11 < l_{xy} < 70$ cm interval is apparent for all m_{Z_D} hypotheses, extending the analysis sensitivity up to $c\tau_0^{Z_D} \gtrsim 1$ m, and enhancing it for $c\tau_0^{Z_D} \gtrsim 10$ mm at small m_{Z_D}.

Within each displacement interval, the events belonging to the pointing category are also categorized according to muon isolation, distinguishing between isolated and nonisolated topologies, and $p_T^{\mu\mu}$. Isolated topologies consist of events where both muons are isolated; nonisolated topologies consist of events where at least one of the two muons fails the isolation criteria defined in Section 5.1. The splitting in isolation aims at covering scenarios where the long-lived particle is created with hadronic activity in its vicinity, such as scalars produced in b hadron decays, and those where the displaced muons are produced alone, such as in $Z_D \to \mu\mu$ decays. Two categories are defined in $p_T^{\mu\mu}$:

- $p_T^{\mu\mu} < 25$ GeV;
- $p_T^{\mu\mu} > 25$ GeV.

The categorization in $p_T^{\mu\mu}$ aims at covering a wide spectrum of possible production scenarios, depending on the particles involved in the process and on their multiplicity. For example, dimuon pairs produced from a decay of a light particle, e.g., a b hadron, have lower $p_T^{\mu\mu}$ than others originating from a much heavier particle, such as a Higgs boson.

A total of 40 dimuon categories are defined, which are considered together with two four-muon categories. In each event category, we define mass windows that slide along the multimuon invariant mass spectrum (as described in Section 6) and perform a search for a resonant peak within each mass window. Mass regions corresponding to known SM resonances decaying either into muon pairs or in a pair of charged hadrons are not considered, i.e., they are "masked". The masked resonances are listed in Table 1. For events with four selected muons, if any of the muon pairs is found within a masked region, this pair is rejected and the event is treated as a dimuon event.

As an example, in Fig. 5 we show the $m_{4\mu}$ spectrum in the multivertex and overlapping vertex categories. In Figs. 6 and 7 (8 and 9), we show the $m_{\mu\mu}$ distribution in bins of l_{xy}, as obtained from selected dimuon events where both muons are isolated and have $p_T^{\mu\mu}$ above (below) 25 GeV.

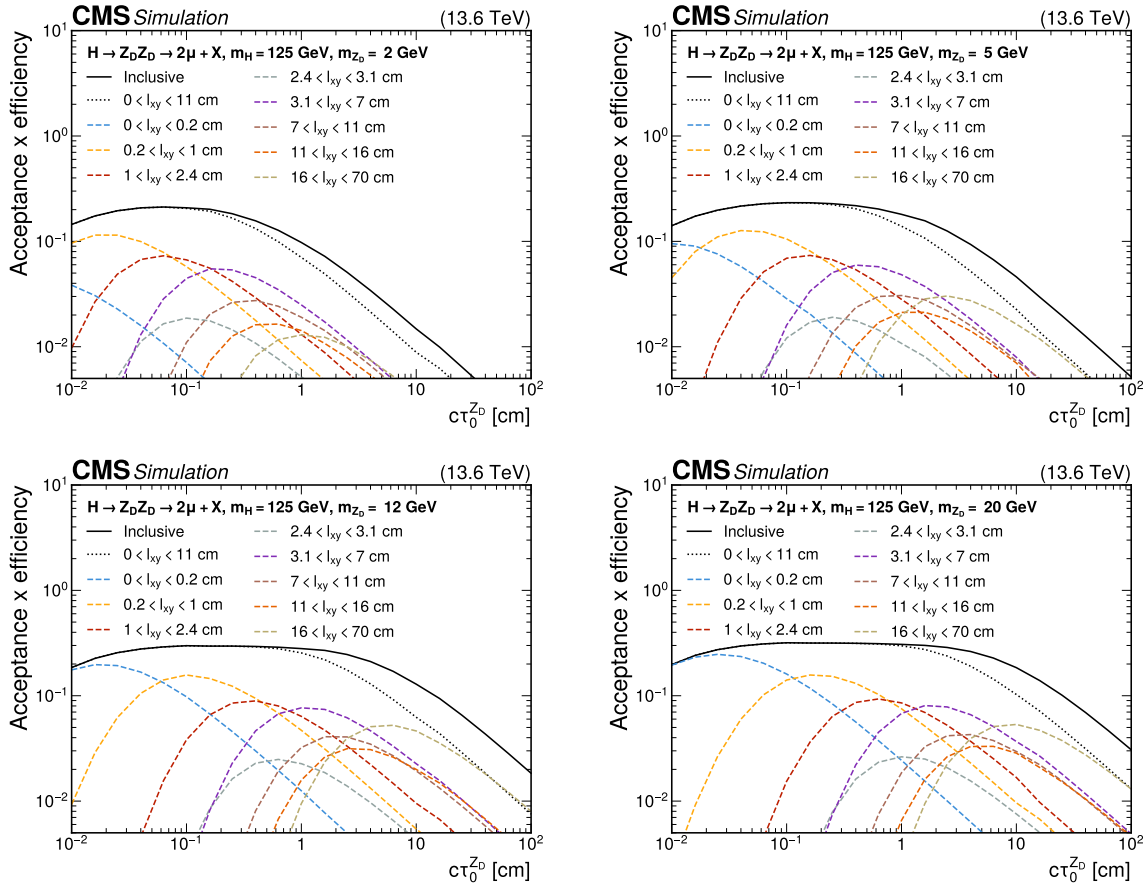

Figure 4: Overall signal acceptance times efficiency ($\mathcal{A}\varepsilon$) as measured for the HAHM signal model with $m_{Z_D} = 2, 5, 12$, and 20 GeV, as a function of the mean proper decay length of the dark photon, $c\tau_0^{Z_D}$. The signal $\mathcal{A}\varepsilon$ is defined as the fraction of events with at least one dark photon decaying into a muon pair, reconstructed as a dimuon candidate within the l_{xy} bins of $[0, 0.2, 1, 2.4, 3.1, 7, 11, 16, 70]$ cm. The average $\mathcal{A}\varepsilon$ over the simulated samples corresponding to the 2022 and 2023 data-taking periods is shown.

Table 1: List of known SM resonances and corresponding masked mass windows, equal to $\pm 5\sigma_{\text{mass}}$ around the mean mass, where mean and resolution (σ_{mass}) are determined from a fit to data.

Resonance	Mean mass [GeV]	σ_{mass} [MeV]	Window [GeV] (mean $\pm$ 5σ_{mass})
K^0_S	0.46	9	[0.41, 0.50]
η	0.55	8	[0.51, 0.59]
$\rho^0(770)/\omega(782)$	0.78	11	[0.73, 0.83]
$\phi(1020)$	1.02	12	[0.96, 1.08]
J/ψ	3.09	35	[2.91, 3.27]
$\psi(2S)$	3.68	42	[3.47, 3.89]
$\Upsilon(1S)$	9.45	93	[8.99, 9.91]
$\Upsilon(2S)$	10.10	91	[9.64, 10.56]
$\Upsilon(3S)$	10.34	87	[9.90, 10.78]

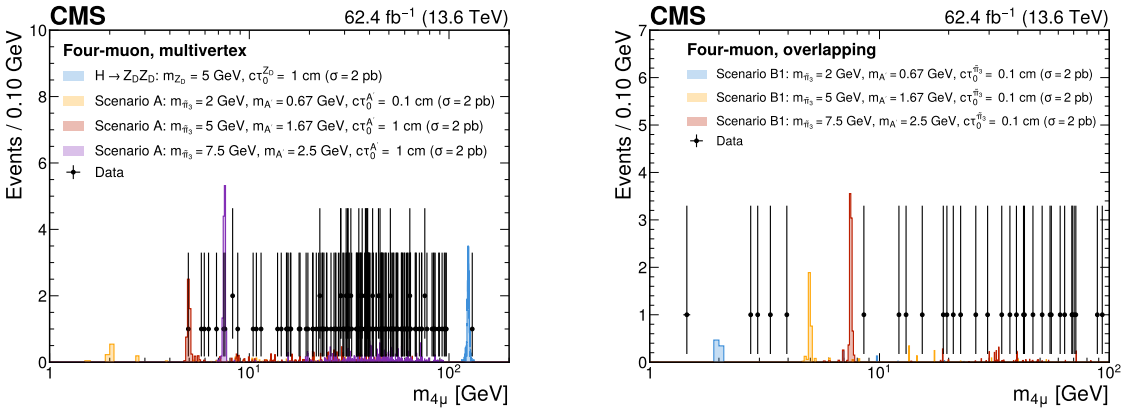

Figure 5: Four-muon invariant mass distributions of selected events in the multivertex (left) and overlapping vertex (right) categories, for data (black points with uncertainties) and representative signal models (colored histograms), assuming a cross section $\sigma = 2\,\text{pb}$ for all models, for visualization purposes.

In each mass window, the SM background is modeled by fitting the multimuon invariant mass distribution in data, as further described in Section 6. Finally, the mass windows in all search bins are used in combination as input to a final likelihood fit for the interpretation of the results, as described in Section 7.

6 Parameterization of the invariant mass distribution

The search is performed by fitting the sum of signal and the SM background models to mass distributions in the various categories, which are separate for the 2022 and 2023 data-taking periods. We target low-mass multimuon resonances whose intrinsic width is assumed to be much narrower than the detector resolution. The signal multimuon invariant mass resolution ($\sigma^{\mu\mu}_{\text{mass}}/m_{\mu\mu} \sim \sigma^{4\mu}_{\text{mass}}/m_{4\mu}$) is estimated from simulated events to be about 1.8% of the mass, with an uncertainty of about 50%, and both are independent of the signal mass and lifetime hypotheses. We use the sum of a Gaussian function and a double-sided Crystal Ball function [46, 47], with common mean and width (σ_{mass}) parameters, to model signal invariant mass distributions in dimuon and 4μ events. The parameters are determined by fitting the corresponding signal MC simulation. Additionally, an interpolation of the signal model parameters is performed between different mass hypotheses to provide a continuous description of the signal shape across the probed mass range.

In each event category, the SM background is modeled in sliding windows of $\pm 5\sigma_{\text{mass}}$ around the considered signal mass hypothesis. These windows are required not to overlap with the masked mass regions corresponding to known SM resonances (as discussed in Section 5.2). A number of functional forms are considered in order to model the background mass distribution. These include Bernstein polynomials, power law, and exponential functions. For each family of functional forms, the best order in each mass window and event category is selected by means of a Fisher test [48]. First, the lowest order (N) function is used to fit the data. Then, the next-order ($N+1$) is used, and the difference $2\Delta\text{NLL}_{N+1} = 2(\text{NLL}_N - \text{NLL}_{N+1})$ (with NLL denoting the negative logarithm of the likelihood of the fit) is evaluated to determine whether the data support the need for a higher-order function. This decision is based on the fact that $2\Delta\text{NLL}_{N+1}$ is asymptotically described by a χ^2 distribution with M degrees of freedom, where M is the difference in the number of free parameters in the $(N+1)$th and Nth order functions

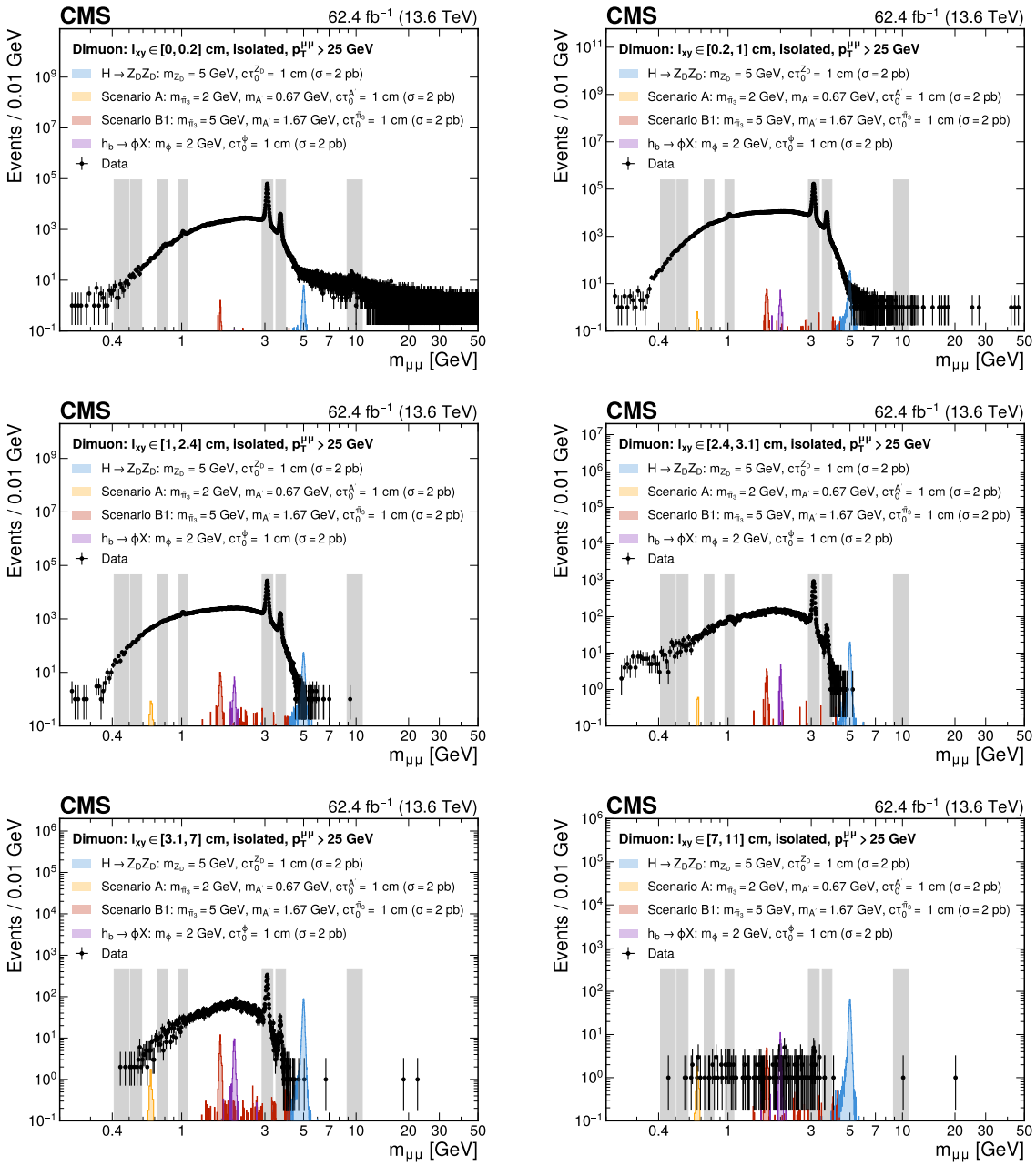

Figure 6: Dimuon invariant mass distributions of selected events with a single, isolated muon pair with $p_{\mathrm{T}}^{\mu\mu} > 25\,\mathrm{GeV}$. Distributions are shown separately for each of the six $l_{\mathrm{xy}} < 11\,\mathrm{cm}$ bins. The vertical gray bands indicate mass ranges containing known SM resonances, which are masked for the purpose of this search. Distributions are shown as obtained in data (black points with uncertainties) and for representative signal models (colored histograms), assuming a cross section $\sigma = 2\,\mathrm{pb}$ for all models, for visualization purposes.

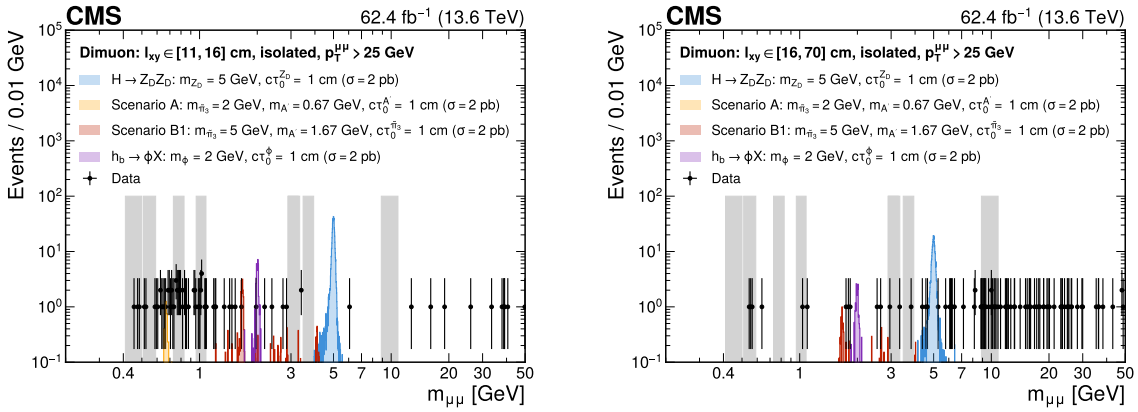

Figure 7: Dimuon invariant mass distributions of selected events with a single, isolated muon pair with $p_T^{\mu\mu} > 25$ GeV. Distributions are shown separately for each of the two $l_{xy} > 11$ cm bins (i.e., for the displacement range inaccessible to the previous results presented in Ref. [20]). The vertical gray bands indicate mass ranges containing known SM resonances, which are masked for the purpose of this search. Distributions are shown as obtained in data (black points with uncertainties) and for representative signal models (colored histograms), assuming a cross section $\sigma = 2$ pb for all models, for visualization purposes.

(in this case $M = 1$). A p-value [49] is calculated as $P_M(\chi^2 > 2\Delta\text{NLL}_{N+1})$ where $P_M(\chi^2_{\text{min}})$ is the χ^2 tail probability for M degrees of freedom. If the p-value is less than 0.05, the higher-order function is retained, since it is determined to significantly improve the description of the data. Once the best order N for each family of functions has been determined, the corresponding functional forms are included in an envelope, which is then used in the discrete profiling method [50], where the choice of the background function is treated as a discrete nuisance parameter in the fit to account for the uncertainty associated with the arbitrary choice of the function. In addition, we use a goodness-of-fit test to remove background models that do not describe the data appropriately. The test is based on a χ^2 test statistic, which is converted into a p-value through a set of pseudo-experiments. Models with $p < 0.01$ are not considered.

The potential presence of a bias in the measurement of a signal due to the choice of the functional forms used to model the SM background is also assessed by means of pseudo-experiments. First, a varying amount of signal is injected on top of the background generated according to the selected functional form. Then, a background + signal fit is performed, allowing the signal yield to float freely. The case of a zero injected signal is also considered. The bias, quantified as the difference between the measured and injected signal yields relative to the statistical uncertainty in the measured signal yield, is found to be negligible.

The background-only fit results for the selected functional forms in one of the dimuon search bins using 2022 data are shown in Fig. 10, as an example, together with the dimuon invariant mass distribution expected for a representative signal hypothesis.

7 Results and interpretation

Unbinned maximum likelihood fits to the data are performed simultaneously in all search bins, under either background-only or background+signal hypotheses, using background and signal models and uncertainties described in Section 6. Additional log-normal constraint terms are used to account for the uncertainties in the signal yields, when considered (Section 7.1).

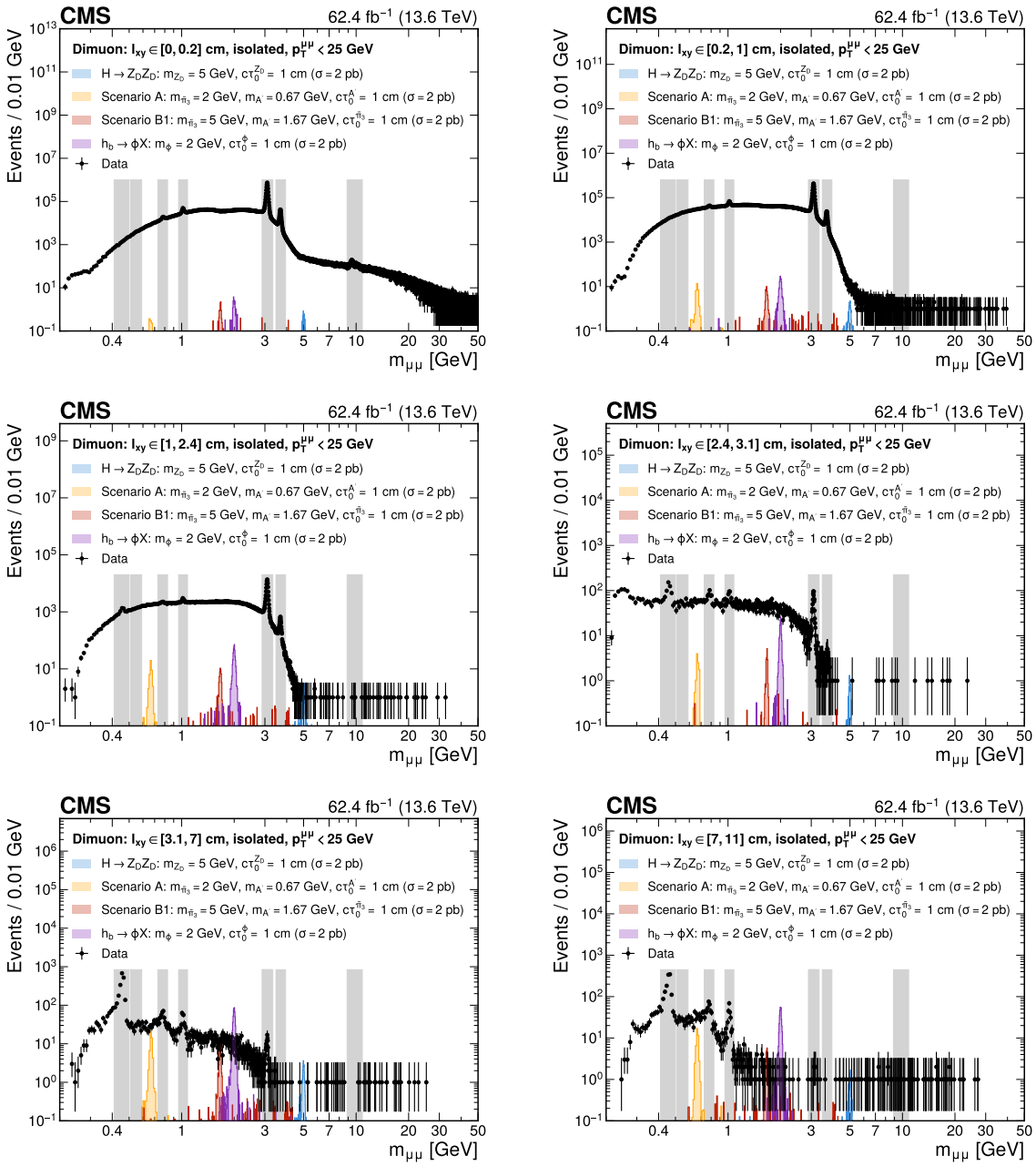

Figure 8: Dimuon invariant mass distributions of selected events with a single, isolated muon pair with $p_{\mathrm{T}}^{\mu\mu} < 25\,\mathrm{GeV}$. Distributions are shown separately for each of the six $l_{\mathrm{xy}} < 11\,\mathrm{cm}$ bins. The vertical gray bands indicate mass ranges containing known SM resonances, which are masked for the purpose of this search. Distributions are shown as obtained in data (black points with uncertainties) and for representative signal models (colored histograms), assuming a cross section $\sigma = 2\,\mathrm{pb}$ for all models, for visualization purposes.

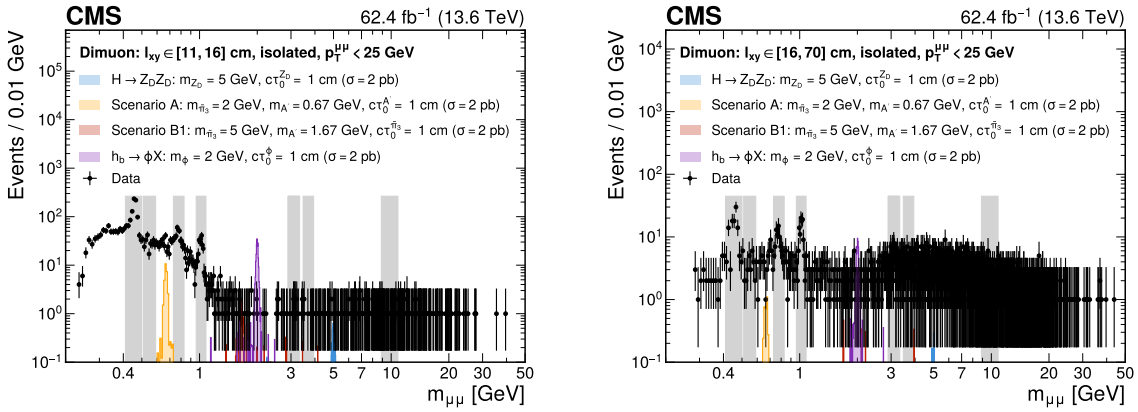

Figure 9: Dimuon invariant mass distributions of selected events with a single, isolated muon pair with $p_T^{\mu\mu} < 25\,\text{GeV}$. Distributions are shown separately for each of the two $l_{xy} > 11\,\text{cm}$ bins (i.e., for the displacement range inaccessible to the previous results presented in Ref. [20]). The vertical gray bands indicate mass ranges containing known SM resonances, which are masked for the purpose of this search. Distributions are shown as obtained in data (black points with uncertainties) and for representative signal models (colored histograms), assuming a cross section $\sigma = 2\,\text{pb}$ for all models, for visualization purposes.

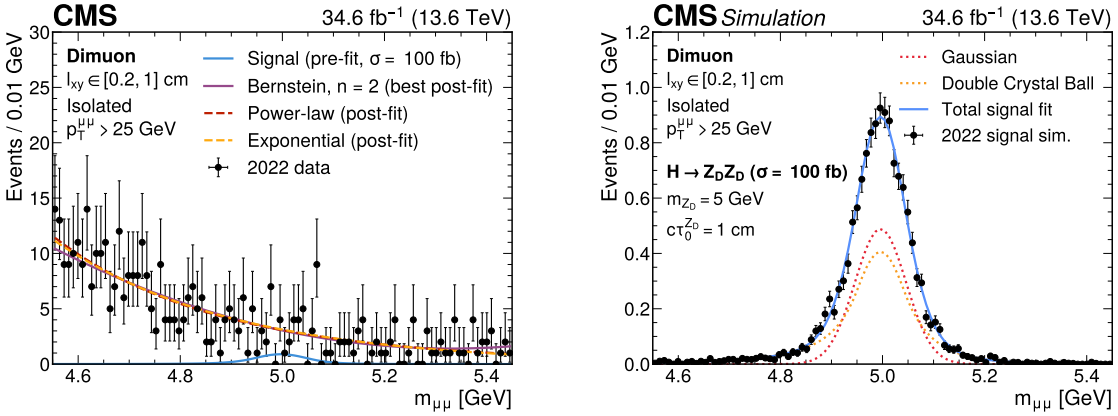

Figure 10: The dimuon invariant mass distribution (left) is shown for data collected in 2022 (black markers) in a mass window centered around 5 GeV, in one of the dimuon search bins ($0.2 < l_{xy} < 1\,\text{cm}$, $p_T^{\mu\mu} > 25\,\text{GeV}$, with two isolated muons). The results of background+signal fits to the data of three selected functional forms are also shown (different colors, partially overlapping lines), highlighting the Bernstein polynomial as the best fit (solid, purple line) for this mass window. The corresponding pre-fit function (solid blue line) for a representative $H \to Z_D Z_D$ signal, with $m_{Z_D} = 5\,\text{GeV}$ and $c\tau_0^{Z_D} = 1\,\text{cm}$, assuming a cross section $\sigma(H \to Z_D Z_D) = 100\,\text{fb}$, is shown for visualization purposes. The fit (solid blue line for the total fit function, and dashed red and orange lines for its individual components) to the dimuon invariant mass distribution (right) expected in the same dimuon search bin is shown for the same signal (black markers).

No significant peak-like structures are observed in data. The background+signal fits are used to set 95% confidence level (CL) upper limits on the branching fractions for the signal models under consideration. Limits are set using a modified frequentist approach, employing the CL_s criterion [51–53] within the CMS statistical analysis tool COMBINE [54], which is based on the ROOFIT [55] and ROOSTATS [56] frameworks. These limits are then used, in conjunction with

the theoretical cross section calculations, to exclude ranges of masses and/or lifetimes for the BSM particles of the signal models.

7.1 Systematic uncertainties in the signal yields

A systematic uncertainty in the trigger efficiency (discussed in Section 3) is assessed to be in the range between 1 and 15%, depending on the p_{T} and displacement of the muons. A separate systematic uncertainty is considered, ranging from 1 to 30% (largest for high-l_{xy} bins), to account for the potential mismodeling of the signal simulation that may introduce a difference in the event selection acceptance for the selection described in Section 5.1. Both uncertainties are derived from studies of $\mathrm{J}/\psi \to \mu^+\mu^-$ data and account for the differences between the measurements in data and simulation. Additionally, we assess a systematic uncertainty in the expected signal yields arising from the uncertainty in the integrated luminosity measurement, of 1.4 (1.3)% for 2022 (2023) data [57–59]. The overall uncertainty in the luminosity measurement for the 2022–2023 period is 1.01%. Finally, we account for uncertainties resulting from the limited size of the simulated signal samples. Uncertainties arising from the choice of the PDFs, and of the renormalization and factorization scales used in the event generators are negligible compared to others. Uncertainties in the trigger efficiency and integrated luminosity are treated as correlated across the search bins. Other uncertainties are taken as uncorrelated. Since we find no significant difference between 2022 and 2023 data and simulations, all uncertainties are treated as correlated across the two data-taking periods.

7.2 Constraints on models of BSM physics

We set upper limits at 95% CL on the branching fraction $\mathcal{B}(\mathrm{H} \to \mathrm{Z_D Z_D})$, using values of $\mathcal{B}(\mathrm{Z_D} \to \mu\mu)$ from the model of Ref. [6]. The constraints we obtain are the most stringent to date for a wide range of signal hypotheses. Upper limits are shown in Fig. 11 as functions of the mass of the dark photon, $m_{\mathrm{Z_D}}$, for dark photon lifetimes $c\tau_0^{\mathrm{Z_D}} = 0.1$, 1, 10, and 100 cm, and in Fig. 12 as functions of the dark photon lifetime for a representative set of $m_{\mathrm{Z_D}}$ hypotheses. We improve and extend the constraints from previous results [20, 22] at small $m_{\mathrm{Z_D}}$ and large $c\tau_0^{\mathrm{Z_D}}$. Compared to Ref. [20], this is achieved despite the smaller amount of available data, thanks to the improved muon scouting triggers, which allow for the reconstruction of displaced muons with $l_{\mathrm{xy}} > 11$ cm, and to the refined event selection and categorization. Compared to Ref. [22], we are able to probe masses $m_{\mathrm{Z_D}} < 10$ GeV, thanks to the lower muon p_{T} thresholds required in the scouting triggers used in this search.

We also set upper limits at 95% CL on the branching fraction $\mathcal{B}(\mathrm{H} \to \Psi\overline{\Psi})$ considering two different dark shower scenarios. Mean proper decay lengths of A′ and $\widetilde{\pi}_3$ ranging from 0.01 to 100 cm are constrained for Scenarios A and B1, respectively. Results are presented in Figs. 13 and 14 for representative mass hypotheses of the dark pion $\widetilde{\pi}_3$ and of the dark photon A′ in Scenarios A and B1, respectively. The results are compared with those previously obtained in Ref. [23], rescaled to the same Higgs boson production cross section of 59.8 pb [40, 41], showing the complementarity of the two analysis strategies. The constraints set in this paper extend the previous limits on the mean proper decay length of the A′ ($\widetilde{\pi}_3$) in Scenario A (B1) in the range from 10 to 100 cm, thanks to the removal of the pixel hit multiplicity requirement in the scouting trigger streams used in this search, extending the sensitivity to larger lifetime hypotheses.

Finally, we set 95% CL upper limits on the branching fraction product $\mathcal{B}(\mathrm{h_b} \to \phi X)\mathcal{B}(\phi \to \mu\mu)$ in a model where a long-lived scalar resonance ϕ arises from the decay of a b hadron. Figure 15 shows the limits obtained as functions of m_ϕ, for $c\tau_0^\phi = 0.1$, 1, and 10 cm. They are found to be mostly consistent with the ones set in Ref. [20], because for such signatures the smaller amount

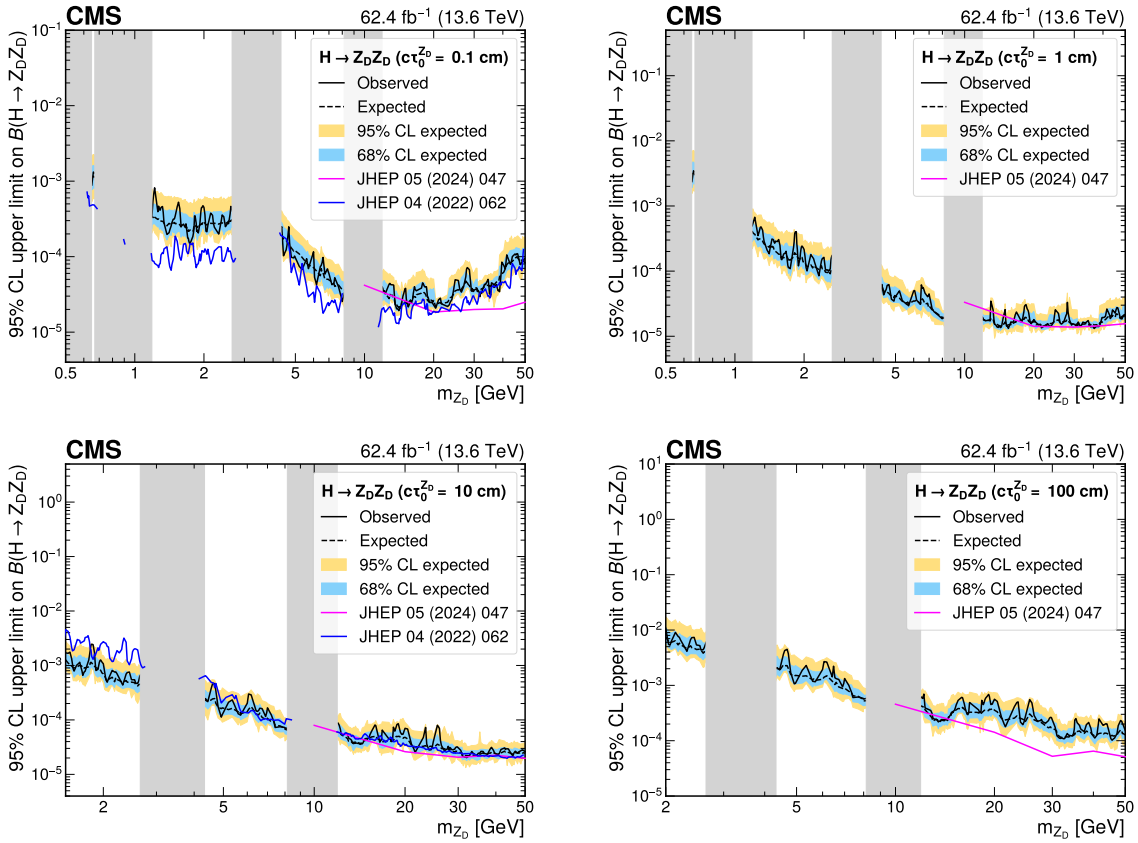

Figure 11: Upper limits at 95% CL on the branching fraction $\mathcal{B}(\mathrm{H} \to \mathrm{Z_D Z_D})$ as functions of the dark-photon mass, $m_{\mathrm{Z_D}}$, for $c\tau_0^{\mathrm{Z_D}} = 0.1$ (upper left), 1 (upper right), 10 (lower left), and 100 cm (lower right). The solid black (dashed black) line represents the observed (median expected) exclusion. The inner blue (outer yellow) band indicates the region containing 68 (95)% of the distribution of limits expected under the background-only hypothesis. The limits are obtained using the combination of all event categories. The dark blue (magenta) solid line represents the observed upper limits previously set in Ref. [20] ([22]). The vertical gray bands indicate mass ranges containing known SM resonances, which are masked for the purpose of this search. The blue (magenta) line can overlap with the gray bands, owing to the different mass ranges covered by the results from Ref. [20] ([22]).

of available data is compensated by the improvements in the scouting triggers and analysis strategy.

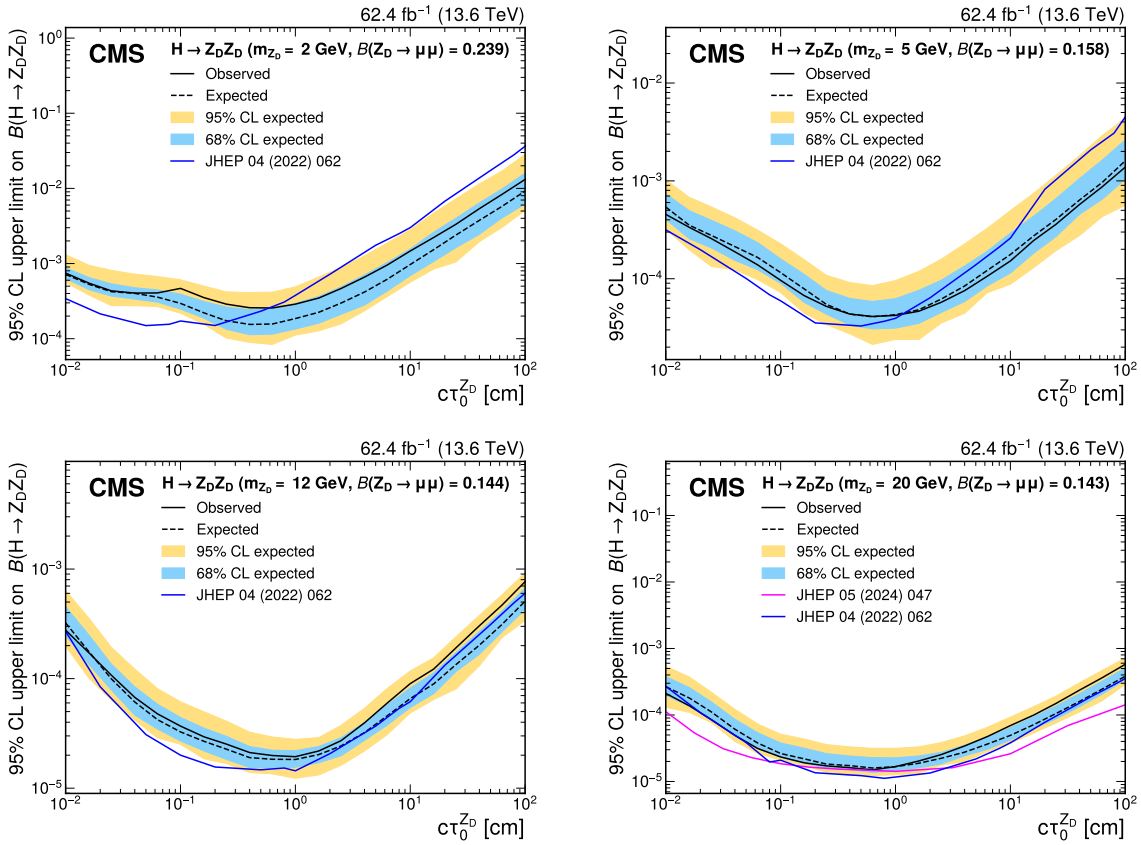

Figure 12: Upper limits at 95% CL on the branching fraction $\mathcal{B}(\mathrm{H} \to \mathrm{Z_D Z_D})$ as functions of $c\tau_0^{\mathrm{Z_D}}$, for representative mass hypotheses, $m_{\mathrm{Z_D}} = 2$ (upper left), 5 (upper right), 12 (lower left), and 20 (lower right) GeV. The solid black (dashed black) line represents the observed (median expected) exclusion. The inner blue (outer yellow) band indicates the region containing 68 (95)% of the distribution of limits expected under the background-only hypothesis. The limits are obtained using the combination of all event categories. The dark blue (magenta) solid line represents the observed upper limits previously set in Ref. [20] ([22]).

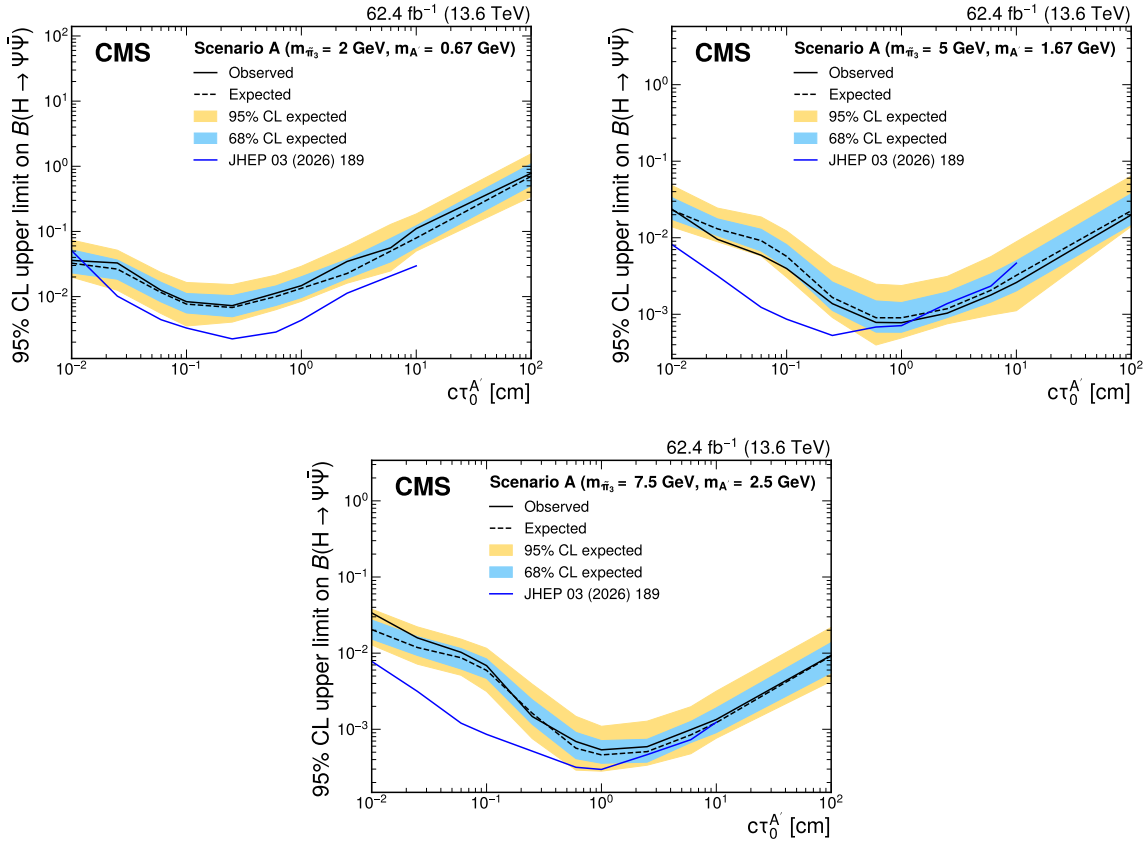

Figure 13: Upper limits at 95% CL on the branching fraction $\mathcal{B}(\mathrm{H} \to \Psi\overline{\Psi})$, for representative mass hypotheses of the Scenario A dark-shower model. Limits are shown as functions of $c\tau_0^{\mathrm{A}'}$, for $m_{\tilde{\pi}} = 2\,\mathrm{GeV}$ and $m_{\mathrm{A}'} = 0.67\,\mathrm{GeV}$ (upper left), $m_{\tilde{\pi}} = 5\,\mathrm{GeV}$ and $m_{\mathrm{A}'} = 1.67\,\mathrm{GeV}$ (upper right), and $m_{\tilde{\pi}} = 7.5\,\mathrm{GeV}$ and $m_{\mathrm{A}'} = 2.5\,\mathrm{GeV}$ (lower). For this model, it is assumed $\tilde{\Lambda} = m_{\tilde{\eta}} = 4m_{\tilde{\pi}}$, $\sin\theta = 0.1$ and $\mathcal{B}(\tilde{\pi}_3 \to \mathrm{A}'\mathrm{A}') = 1$. The solid black (dashed black) line represents the observed (median expected) exclusion. The inner blue (outer yellow) band indicates the region containing 68 (95)% of the distribution of limits expected under the background-only hypothesis. The limits are obtained using the combination of all event categories. The dark blue solid line represents the observed upper limits previously set in Ref. [23], rescaled to the same Higgs boson production cross section of 59.8 pb [40, 41].

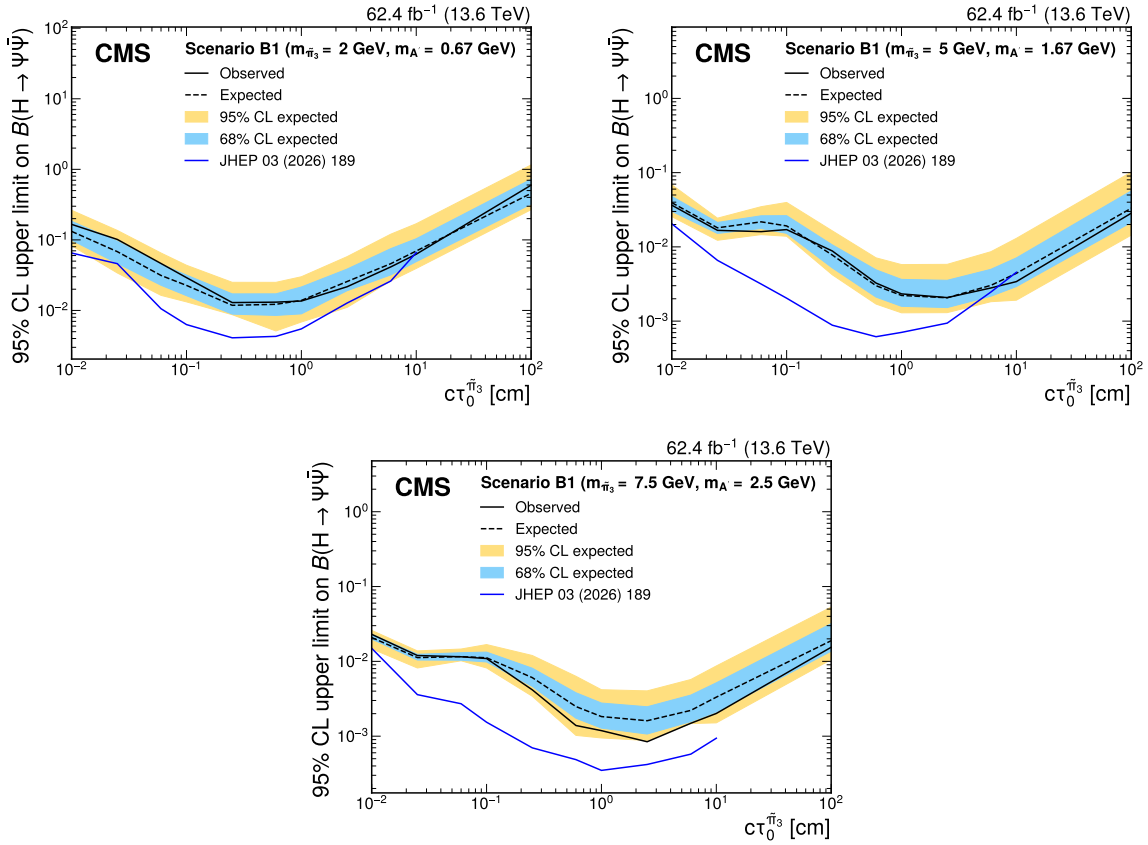

Figure 14: Upper limits at 95% CL on the branching fraction $\mathcal{B}(\mathrm{H} \to \Psi\overline{\Psi})$, for representative mass hypotheses of the Scenario B1 dark-shower model. Limits are shown as functions of $c\tau_0^{\widetilde{\pi}_3}$, for $m_{\widetilde{\pi}} = 2\,\mathrm{GeV}$ and $m_{\mathrm{A}'} = 0.67\,\mathrm{GeV}$ (upper left), $m_{\widetilde{\pi}} = 5\,\mathrm{GeV}$ and $m_{\mathrm{A}'} = 1.67\,\mathrm{GeV}$ (upper right), and $m_{\widetilde{\pi}} = 7.5\,\mathrm{GeV}$ and $m_{\mathrm{A}'} = 2.5\,\mathrm{GeV}$ (lower). For this model, it is assumed $\tilde{\Lambda} = m_{\widetilde{\eta}} = 4m_{\widetilde{\pi}}$, $\sin\theta = 0.1$ and $\mathcal{B}(\widetilde{\pi}_3 \to \mathrm{A}'\mathrm{A}') = 1$. The solid black (dashed black) line represents the observed (median expected) exclusion. The inner blue (outer yellow) band indicates the region containing 68 (95)% of the distribution of limits expected under the background-only hypothesis. The limits are obtained using the combination of all event categories. The dark blue solid line represents the observed upper limits previously set in Ref. [23], rescaled to the same Higgs boson production cross section of 59.8 pb [40, 41].

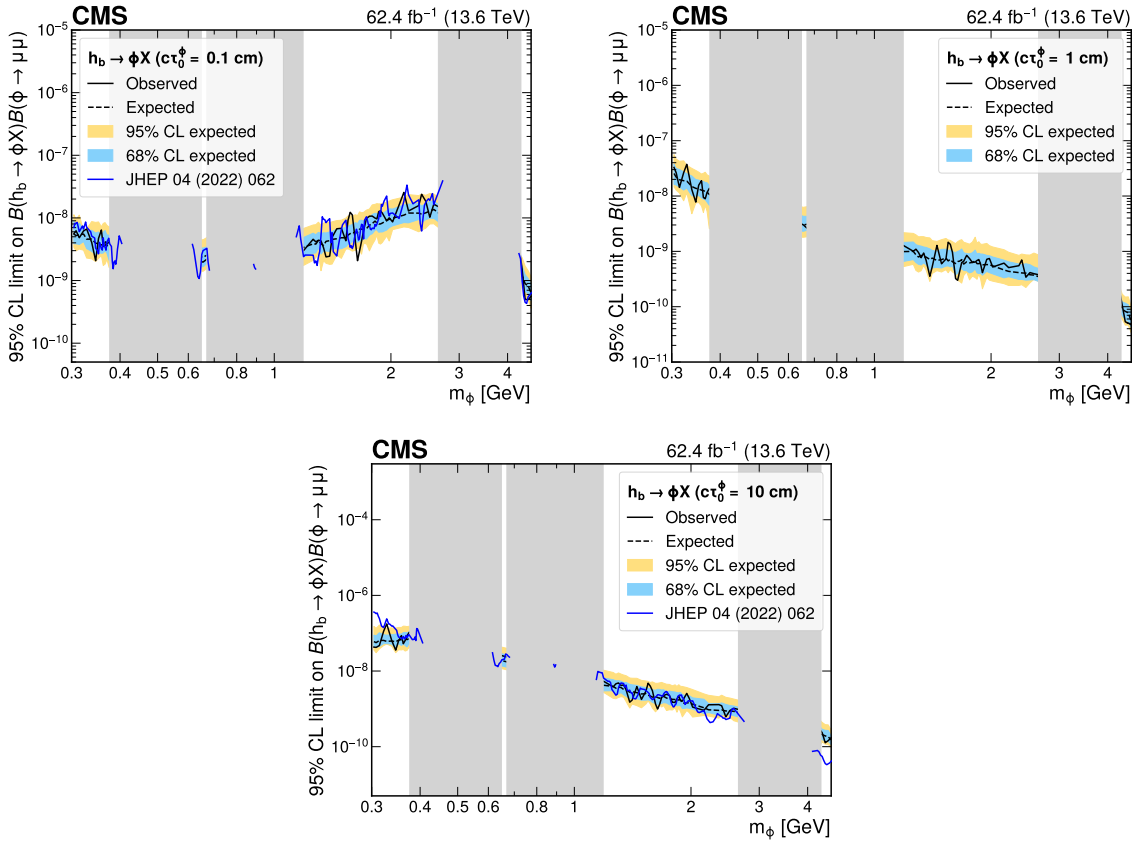

Figure 15: Upper limits at 95% CL on the branching fraction product $\mathcal{B}(\mathrm{h_b} \to \phi X)\mathcal{B}(\phi \to \mu\mu)$ as functions of the long-lived scalar resonance mass, m_ϕ, for $c\tau_0^\phi = 0.1$ (upper left), 1 (upper right), and 10 cm (lower). The solid black (dashed black) line represents the observed (median expected) exclusion. The inner blue (outer yellow) band indicates the region containing 68 (95)% of the distribution of limits expected under the background-only hypothesis. The limits are obtained using the combination of all dimuon event categories. The dark blue solid line represents the exclusion limits previously set in Ref. [20]. The vertical gray bands indicate mass ranges containing known SM resonances, which are masked for the purpose of this search. The blue line can overlap with the gray bands, owing to the different mass ranges covered by the results from Ref. [20].

8 Summary

A search for displaced multimuon resonances has been performed using proton-proton collisions at a center-of-mass energy of 13.6 TeV, collected by the CMS experiment at the LHC in 2022 and 2023, corresponding to an integrated luminosity of 62.4 fb^{-1}. The data were collected using a dedicated dimuon trigger stream with low transverse momentum thresholds, recorded at high rate by retaining a reduced amount of information at the high-level trigger, to explore otherwise inaccessible phase space at low multimuon invariant mass and nonzero displacement from the primary interaction vertex. No significant excess above the standard model prediction is found. The data are used to set constraints on a wide range of mass and lifetime hypotheses for various scenarios of physics beyond the standard model. Three sets of models are considered: the hidden Abelian Higgs model, where the Higgs boson decays into a pair of long-lived dark photons; dark-shower models, where dark showers originate from the Higgs boson decays into dark quarks; and models where a long-lived scalar resonance is produced from the decay of a b hadron. In the hidden Abelian Higgs model, the most stringent limits to date are obtained for dark-photon proper decay lengths greater than 1 cm and dark-photon masses less than 5 GeV. In the dark-shower models, the most stringent limits to date are set for proper decay lengths larger than 10 cm. In models with a b hadron, the improved trigger and analysis strategy compensate for the smaller data set, leading to constraints comparable to the previous results.

Acknowledgments

We congratulate our colleagues in the CERN accelerator departments for the excellent performance of the LHC and thank the technical and administrative staffs at CERN and at other CMS institutes for their contributions to the success of the CMS effort. In addition, we gratefully acknowledge the computing centers and personnel of the Worldwide LHC Computing Grid and other centers for delivering so effectively the computing infrastructure essential to our analyses. Finally, we acknowledge the enduring support for the construction and operation of the LHC, the CMS detector, and the supporting computing infrastructure provided by the following funding agencies: SC (Armenia), BMBWF and FWF (Austria); FNRS and FWO (Belgium); CNPq, CAPES, FAPERJ, FAPERGS, and FAPESP (Brazil); MES and BNSF (Bulgaria); CERN; CAS, MoST, and NSFC (China); MINCIENCIAS (Colombia); MSES and CSF (Croatia); RIF (Cyprus); SENESCYT (Ecuador); ERC PRG and PSG, TARISTU24-TK10 and MoER TK202 (Estonia); Academy of Finland, MEC, and HIP (Finland); CEA and CNRS/IN2P3 (France); SRNSF (Georgia); BMFTR, DFG, and HGF (Germany); GSRI (Greece); MATE and NKFIH (Hungary); DAE and DST (India); IPM (Iran); SFI (Ireland); INFN (Italy); MSIT and NRF (Republic of Korea); MES (Latvia); LMTLT (Lithuania); MOE and UM (Malaysia); BUAP, CINVESTAV, CONACYT, LNS, SEP, and UASLP-FAI (Mexico); MOS (Montenegro); MBIE (New Zealand); PAEC (Pakistan); MSHE, NSC, and NAWA (Poland); FCT (Portugal); MESTD (Serbia); MICIU/AEI and PCTI (Spain); MOSTR (Sri Lanka); Swiss Funding Agencies (Switzerland); MST (Taipei); MHESI (Thailand); TUBITAK and TENMAK (Türkiye); NASU (Ukraine); STFC (United Kingdom); DOE and NSF (USA).

Individuals have received support from the Marie-Curie program and the European Research Council and Horizon 2020 Grant, contract Nos. 675440, 724704, 752730, 758316, 765710, 824093, 101115353, 101002207, 101001205, and COST Action CA16108 (European Union); the Leventis Foundation; the Alfred P. Sloan Foundation; the Alexander von Humboldt Foundation; the Science Committee, project no. 22rl-037 (Armenia); the Fonds pour la Formation à la Recherche dans l'Industrie et dans l'Agriculture (FRIA) and Fonds voor Wetenschappelijk On-

derzoek contract No. 1228724N (Belgium); the Beijing Municipal Science & Technology Commission, No. Z191100007219010, the Fundamental Research Funds for the Central Universities, the Ministry of Science and Technology of China under Grant No. 2023YFA1605804, the Natural Science Foundation of China under Grant No. 12535004, and USTC Research Funds of the Double First-Class Initiative No. YD2030002017 (China); the Ministry of Education, Youth and Sports (MEYS) of the Czech Republic; the Shota Rustaveli National Science Foundation (Georgia); the Deutsche Forschungsgemeinschaft (DFG), among others, under Germany's Excellence Strategy – EXC 2121 "Quantum Universe" – 390833306, and under project number 400140256 - GRK2497; the Hellenic Foundation for Research and Innovation (HFRI), Project Number 2288 (Greece); the Hungarian Academy of Sciences, the New National Excellence Program - ÚNKP, the NKFIH research grants K 131991, K 138136, K 143460, K 143477, K 147557, K 146913, K 146914, K 147048, TKP2021-NKTA-64, and 2025-1.1.5-NEMZ_KI-2025-00004, and MATE KKP and KKPCs Research Excellence and Flagship Research Groups grants (Hungary); the Council of Science and Industrial Research, India; ICSC – National Research Center for High Performance Computing, Big Data and Quantum Computing, FAIR – Future Artificial Intelligence Research, and CUP I53D23001070006 (Mission 4 Component 1), funded by the NextGenerationEU program, the Italian Ministry of University and Research (MUR) under Bando PRIN 2022 – CUP I53C24002390006, PRIN PRIMULA 2022RBYK7T (Italy); the Latvian Council of Science; the Ministry of Science and Higher Education, project no. 2022/WK/14, and the National Science Center, contracts Opus 2021/41/B/ST2/01369, 2021/43/B/ST2/01552, 2023/49/B/ST2/03273, and the NAWA contract BPN/PPO/2021/1/00011 (Poland); the Fundação para a Ciência e a Tecnologia (Portugal); the National Priorities Research Program by Qatar National Research Fund; MICIU/AEI/10.13039/501100011033, ERDF/EU, "European Union NextGenerationEU/PRTR", projects PID2022-142604OB-C21, PID2022-139519OB-C21, PID2023-147706NB-I00, PID2023-148896NB-I00, PID2023-146983NB-I00, PID2023-147115NB-I00, PID2023-148418NB-C41, PID2023-148418NB-C42, PID2023-148418NB-C43, PID2023-148418NB-C44, PID2024-158190NB-C22, RYC2021-033305-I, RYC2024-048719-I, CNS2023-144781, CNS2024-154769 and Plan de Ciencia, Tecnología e Innovación de Asturias, Spain; the Chulalongkorn Academic into Its 2nd Century Project Advancement Project, the National Science, Research and Innovation Fund program IND_FF_68_369_2300_097, and the Program Management Unit for Human Resources & Institutional Development, Research and Innovation, grant B39G680009 (Thailand); the Eric & Wendy Schmidt Fund for Strategic Innovation through the CERN Next Generation Triggers project under grant agreement number SIF-2023-004; the Kavli Foundation; the Nvidia Corporation; the SuperMicro Corporation; the Welch Foundation, contract C-1845; and the Weston Havens Foundation (USA).

References

[1] G. Bertone and J. Silk, "Particle dark matter: Observations, models and searches". Cambridge Univ. Press, Cambridge, 2010. doi:10.1017/CBO9780511770739, ISBN 978-1-107-65392-4.

[2] J. L. Feng, "Dark matter candidates from particle physics and methods of detection", *Ann. Rev. Astron. Astrophys.* **48** (2010) 495, doi:10.1146/annurev-astro-082708-101659, arXiv:1003.0904.

[3] T. A. Porter, R. P. Johnson, and P. W. Graham, "Dark matter searches with astroparticle data", *Ann. Rev. Astron. Astrophys.* **49** (2011) 155, doi:10.1146/annurev-astro-081710-102528, arXiv:1104.2836.

[4] Planck Collaboration, "Planck 2015 results. XIII. Cosmological parameters", *Astron. Astrophys.* **594** (2016) A13, doi:10.1051/0004-6361/201525830, arXiv:1502.01589.

[5] R. Essig et al., "Working group report: New light weakly coupled particles", in *Proc. Community Summer Study 2013: Snowmass on the Mississippi*. 2013. arXiv:1311.0029.

[6] D. Curtin, R. Essig, S. Gori, and J. Shelton, "Illuminating dark photons with high-energy colliders", *JHEP* **02** (2015) 157, doi:10.1007/JHEP02(2015)157, arXiv:1412.0018.

[7] CMS Collaboration, "Dark sector searches with the CMS experiment", *Phys. Rept.* **1115** (2025) 448, doi:10.1016/j.physrep.2024.09.013, arXiv:2405.13778.

[8] S. Born, R. Karur, S. Knapen, and J. Shelton, "Scouting for dark showers at CMS and LHCb", *Phys. Rev. D* **108** (2023) 035034, doi:10.1103/PhysRevD.108.035034, arXiv:2303.04167.

[9] A. Konaka et al., "Search for neutral particles in electron beam dump experiment", *Phys. Rev. Lett.* **57** (1986) 659, doi:10.1103/PhysRevLett.57.659.

[10] APEX Collaboration, "Search for a new gauge boson in electron-nucleus fixed-target scattering by the APEX experiment", *Phys. Rev. Lett.* **107** (2011) 191804, doi:10.1103/PhysRevLett.107.191804, arXiv:1108.2750.

[11] BaBar Collaboration, "Search for dimuon decays of a light scalar boson in radiative transitions $\Upsilon \to \gamma A^0$", *Phys. Rev. Lett.* **103** (2009) 081803, doi:10.1103/PhysRevLett.103.081803, arXiv:0905.4539.

[12] SINDRUM I Collaboration, "Search for weakly interacting neutral bosons produced in π^-p interactions at rest and decaying into e^+e^- pairs", *Phys. Rev. Lett.* **68** (1992) 3845, doi:10.1103/PhysRevLett.68.3845.

[13] LHCb Collaboration, "Proposed inclusive dark photon search at LHCb", *Phys. Rev. Lett.* **116** (2016) 251803, doi:10.1103/PhysRevLett.116.251803, arXiv:1603.08926.

[14] LHCb Collaboration, "Search for dark photons produced in 13 TeV pp collisions", *Phys. Rev. Lett.* **120** (2018) 061801, doi:10.1103/PhysRevLett.120.061801, arXiv:1710.02867.

[15] LHCb Collaboration, "Search for $A' \to \mu^+\mu^-$ decays", *Phys. Rev. Lett.* **124** (2020) 041801, doi:10.1103/PhysRevLett.124.041801, arXiv:1910.06926.

[16] ATLAS Collaboration, "Search for light long-lived neutral particles that decay to collimated pairs of leptons or light hadrons in pp collisions at $\sqrt{s} = 13$ TeV with the ATLAS detector", *JHEP* **06** (2023) 153, doi:10.1007/JHEP06(2023)153, arXiv:2206.12181.

[17] ATLAS Collaboration, "Search for light long-lived neutral particles from Higgs boson decays via vector-boson-fusion production from pp collisions at $\sqrt{s} = 13$ TeV with the ATLAS detector", *Eur. Phys. J. C* **84** (2024) 719, doi:10.1140/epjc/s10052-024-12902-7, arXiv:2311.18298.

[18] ATLAS Collaboration, "Search for events with one displaced vertex from long-lived neutral particles decaying into hadronic jets in the ATLAS muon spectrometer in pp collisions at $\sqrt{s} = 13$ TeV", *Phys. Rev. D* **112** (2025) 092001, doi:10.1103/cmql-s9sq, arXiv:2503.20445.

[19] CMS Collaboration, "Search for a narrow resonance lighter than 200 GeV decaying to a pair of muons in proton-proton collisions at $\sqrt{s} = 13$ TeV", *Phys. Rev. Lett.* **124** (2020) 131802, doi:10.1103/PhysRevLett.124.131802, arXiv:1912.04776.

[20] CMS Collaboration, "Search for long-lived particles decaying into muon pairs in proton-proton collisions at $\sqrt{s} = 13$ TeV collected with a dedicated high-rate data stream", *JHEP* **04** (2022) 062, doi:10.1007/JHEP04(2022)062, arXiv:2112.13769.

[21] CMS Collaboration, "Search for direct production of GeV-scale resonances decaying to a pair of muons in proton-proton collisions at $\sqrt{s} = 13$ TeV", *JHEP* **12** (2023) 070, doi:10.1007/JHEP12(2023)070, arXiv:2309.16003.

[22] CMS Collaboration, "Search for long-lived particles decaying to final states with a pair of muons in proton-proton collisions at $\sqrt{s} = 13.6$ TeV", *JHEP* **05** (2024) 047, doi:10.1007/JHEP05(2024)047, arXiv:2402.14491.

[23] CMS Collaboration, "Search for low-mass hidden-valley dark showers with non-prompt muon pairs in proton-proton collisions at $\sqrt{s} = 13$ TeV", *JHEP* **03** (2026) 189, doi:10.1007/JHEP03(2026)189, arXiv:2511.11888.

[24] F. Bezrukov and D. Gorbunov, "Light inflaton after LHC8 and WMAP9 results", *JHEP* **07** (2013) 140, doi:10.1007/JHEP07(2013)140, arXiv:1303.4395.

[25] J. A. Evans, A. Gandrakota, S. Knapen, and H. Routray, "Searching for exotic B meson decays with the CMS L1 track trigger", *Phys. Rev. D* **103** (2021) 015026, doi:10.1103/PhysRevD.103.015026, arXiv:2008.06918.

[26] CHARM Collaboration, "Search for axion like particle production in 400 GeV proton-copper interactions", *Phys. Lett. B* **157** (1985) 458, doi:10.1016/0370-2693(85)90400-9.

[27] LHCb Collaboration, "Search for hidden-sector bosons in $B^0 \to K^{*0}\mu^+\mu^-$ decays", *Phys. Rev. Lett.* **115** (2015) 161802, doi:10.1103/PhysRevLett.115.161802, arXiv:1508.04094.

[28] LHCb Collaboration, "Search for long-lived scalar particles in $B^+ \to K^+\chi\,(\mu^+\mu^-)$ decays", *Phys. Rev. D* **95** (2017) 071101, doi:10.1103/PhysRevD.95.071101, arXiv:1612.07818.

[29] CMS Collaboration, "Enriching the physics program of the CMS experiment via data scouting and data parking", *Phys. Rept.* **1115** (2025) 678, doi:10.1016/j.physrep.2024.09.006, arXiv:2403.16134.

[30] HEPData record for this analysis, 2026. doi:10.17182/hepdata.169181.

[31] CMS Collaboration, "Particle-flow reconstruction and global event description with the CMS detector", *JINST* **12** (2017) P10003, doi:10.1088/1748-0221/12/10/P10003, arXiv:1706.04965.

[32] Tracker Group of the CMS Collaboration, "The CMS phase-1 pixel detector upgrade", *JINST* **16** (2021) P02027, doi:10.1088/1748-0221/16/02/P02027, arXiv:2012.14304.

[33] CMS Collaboration, "The CMS experiment at the CERN LHC", *JINST* **3** (2008) S08004, doi:10.1088/1748-0221/3/08/S08004.

[34] CMS Collaboration, "Development of the CMS detector for the CERN LHC Run 3", *JINST* **19** (2024) P05064, doi:10.1088/1748-0221/19/05/P05064, arXiv:2309.05466.

[35] CMS Collaboration, "Performance of the CMS Level-1 trigger in proton-proton collisions at $\sqrt{s} = 13\,\text{TeV}$", *JINST* **15** (2020) P10017, doi:10.1088/1748-0221/15/10/P10017, arXiv:2006.10165.

[36] CMS Collaboration, "The CMS trigger system", *JINST* **12** (2017) P01020, doi:10.1088/1748-0221/12/01/P01020, arXiv:1609.02366.

[37] CMS Collaboration, "Performance of the CMS high-level trigger during LHC Run 2", *JINST* **19** (2024) P11021, doi:10.1088/1748-0221/19/11/P11021, arXiv:2410.17038.

[38] CMS Collaboration, "Strategy and performance of the CMS long-lived particle trigger program in proton-proton collisions at $\sqrt{s} = 13.6\,\text{TeV}$", 2026. arXiv:2601.17544. Submitted to *Phys. Rept.*

[39] J. Alwall et al., "The automated computation of tree-level and next-to-leading order differential cross sections, and their matching to parton shower simulations", *JHEP* **07** (2014) 079, doi:10.1007/JHEP07(2014)079, arXiv:1405.0301.

[40] M. Cepeda et al., "Report from working group 2: Higgs physics at the HL-LHC and HE-LHC", *CERN Yellow Rep. Monogr.* **7** (2019) 221, doi:10.23731/CYRM-2019-007.221, arXiv:1902.00134.

[41] A. Karlberg et al., "Ad interim recommendations for the Higgs boson production cross sections at $\sqrt{s} = 13.6\,\text{TeV}$", 2024. arXiv:2402.09955.

[42] C. Bierlich et al., "A comprehensive guide to the physics and usage of PYTHIA 8.3", *SciPost Phys. Codeb.* **2022** (2022) 8, doi:10.21468/SciPostPhysCodeb.8, arXiv:2203.11601.

[43] CMS Collaboration, "Extraction and validation of a new set of CMS PYTHIA 8 tunes from underlying-event measurements", *Eur. Phys. J. C* **80** (2020) 4, doi:10.1140/epjc/s10052-019-7499-4, arXiv:1903.12179.

[44] NNPDF Collaboration, "Parton distributions from high-precision collider data", *Eur. Phys. J. C* **77** (2017) 663, doi:10.1140/epjc/s10052-017-5199-5, arXiv:1706.00428.

[45] GEANT4 Collaboration, "GEANT4—a simulation toolkit", *Nucl. Instrum. Meth. A* **506** (2003) 250, doi:10.1016/S0168-9002(03)01368-8.

[46] M. J. Oreglia, "A study of the reactions $\psi' \to \gamma\gamma\psi$". PhD thesis, Stanford University, 1980. SLAC Report SLAC-R-236, see Appendix D.

[47] J. E. Gaiser, "Charmonium spectroscopy from radiative decays of the J/ψ and ψ'". PhD thesis, Stanford University, 1982. SLAC Report SLAC-R-255.

[48] R. A. Fisher, "On the interpretation of χ^2 from contingency tables, and the calculation of P", *J. R. Stat. Soc* **85** (1922) 87, doi:10.1098/rsta.1922.0009.

[49] E. Gross and O. Vitells, "Trial factors for the look elsewhere effect in high energy physics", *Eur. Phys. J. C* **70** (2010) 525, doi:10.1140/epjc/s10052-010-1470-8, arXiv:1005.1891.

[50] P. D. Dauncey, M. Kenzie, N. Wardle, and G. J. Davies, "Handling uncertainties in background shapes: the discrete profiling method", *JINST* **10** (2015) P04015, doi:10.1088/1748-0221/10/04/P04015, arXiv:1408.6865.

[51] T. Junk, "Confidence level computation for combining searches with small statistics", *Nucl. Instrum. Meth. A* **434** (1999) 435, doi:10.1016/S0168-9002(99)00498-2, arXiv:hep-ex/9902006.

[52] A. L. Read, "Presentation of search results: The CL_s technique", *J. Phys. G* **28** (2002) 2693, doi:10.1088/0954-3899/28/10/313.

[53] ATLAS and CMS Collaborations, "Procedure for the LHC Higgs boson search combination in summer 2011", ATL-PHYS-PUB-2011-011, CMS NOTE-2011/005, 2011.

[54] CMS Collaboration, "The CMS statistical analysis and combination tool: COMBINE", *Comput. Softw. Big Sci.* **8** (2024) 19, doi:10.1007/s41781-024-00121-4, arXiv:2404.06614.

[55] W. Verkerke and D. Kirkby, "The ROOFIT toolkit for data modeling", in *Proc. 13th International Conference on Computing in High Energy and Nuclear Physics (CHEP 2003): La Jolla CA, United States, March 24–28, 2003*. 2003. arXiv:physics/0306116.

[56] L. Moneta et al., "The ROOSTATS project", in *Proc. 13th International Workshop on Advanced Computing and Analysis Techniques in Physics Research (ACAT 2010): Jaipur, India, February 22–27, 2010*. 2010. arXiv:1009.1003. doi:10.22323/1.093.0057.

[57] CMS Collaboration, "Precision luminosity measurement in proton-proton collisions at $\sqrt{s} = 13$ TeV in 2015 and 2016 at CMS", *Eur. Phys. J. C* **81** (2021) 800, doi:10.1140/epjc/s10052-021-09538-2, arXiv:2104.01927.

[58] CMS Collaboration, "Luminosity measurement in proton-proton collisions at 13.6 TeV in 2022 at CMS", CMS Physics Analysis Summary, CMS-PAS-LUM-22-001, 2024.

[59] CMS Collaboration, "Measurement of the offline integrated luminosity for the CMS proton-proton collision dataset recorded in 2023", CMS Detector Performance Note, CMS-DP-2024-068, 2024.

A The CMS Collaboration

Yerevan Physics Institute, Yerevan, Armenia
A. Gevorgyan, A. Hayrapetyan, V. Makarenko, A. Tumasyan[1]

Marietta Blau Institute for Particle Physics, Vienna, Austria
W. Adam, L. Benato, T. Bergauer, M. Dragicevic, S. Gundacker, A.K. Guven, P.S. Hussain, M. Jeitler[2], N. Krammer, A. Li, D. Liko, M. Matthewman, J. Schieck[2], R. Schöfbeck[2], M. Shooshtari, M. Sonawane, N. Van Den Bossche, W. Waltenberger, C.E. Wulz[2]

Universiteit Antwerpen, Antwerpen, Belgium
T. Janssen, D. Ocampo Henao, T. Van Laer, P. Van Mechelen

Vrije Universiteit Brussel, Brussel, Belgium
D. Ahmadi, J. Bierkens, N. Breugelmans, S. Dansana, A. De Moor, M. Delcourt, S. Duponcheel, C. Gupta, F. Heyen, Y. Hong, K. Kang, P. Kashko, S. Lowette, I. Makarenko, S. Nandakumar, S. Tavernier, M. Tytgat[3], G.P. Van Onsem, S. Van Putte, T. Wybouw

Université Libre de Bruxelles, Bruxelles, Belgium
A. Beshr, B. Bilin, F. Caviglia Roman, B. Clerbaux, A.K. Das, I. De Bruyn, G. De Lentdecker, E. Ducarme, H. Evard, L. Favart, I. Kalaitzidou, A. Khalilzadeh, A. Malara, M.A. Shahzad, L. Thomas, M. Vanden Bemden, C. Vander Velde, P. Vanlaer, C. Yuan, F. Zhang

Ghent University, Ghent, Belgium
A. Cauwels, M. De Coen, D. Dobur, C. Giordano, G. Gokbulut, K. Kaspar, D. Kavtaradze, D. Marckx, A. Mehta, K. Skovpen, A.M. Tomaru, J. van der Linden, J. Vandenbroeck

Université Catholique de Louvain, Louvain-la-Neuve, Belgium
H. Aarup Petersen, A. Benecke, A. Bethani, G. Bruno, A. Cappati, J. De Favereau De Jeneret, C. Delaere, F. Gameiro Casalinho, A. Giammanco, A.O. Guzel, M. Hussain, Z. Lawrence, V. Lemaitre, J. Lidrych, P. Malek, S. Turkcapar

Centro Brasileiro de Pesquisas Fisicas, Rio de Janeiro, Brazil
G. Alves, M. Barroso Ferreira Filho, E. Coelho, M.V. Gonçalves Sales, C. Hensel, D. Matos Figueiredo, T. Menezes De Oliveira, C. Mora Herrera, P. Rebello Teles, M. Soeiro, E.J. Tonelli Manganote[4], A. Vilela Pereira

Universidade do Estado do Rio de Janeiro, Rio de Janeiro, Brazil
W.L. Aldá Júnior, H. Brandao Malbouisson, W. Carvalho, J. Chinellato[5], G. Correia Silva, M. Costa Reis, E.M. Da Costa, D. Da Silva Dalto, G.G. Da Silveira[6], D. De Jesus Damiao, S. Fonseca De Souza, R. Gomes De Souza, S. Jesus, T. Laux Kuhn[6], K. Maslova Gioseffi Defante, K. Mota Amarilo, L. Mundim, H. Nogima, J.P. Pinheiro, A. Santoro, A. Sznajder, M. Thiel, F. Torres Da Silva De Araujo[7], D. Torres Machado

Universidade Estadual Paulista (a), Universidade Federal do ABC (b), São Paulo, Brazil
C.A. Bernardes, L. Calligaris, J. Carvalho Leite, F. Damas, E. De Moraes Gregores, B. Lopes Da Costa, I. Maietto Silverio, P.G. Mercadante, S.F. Novaes, S. Padula, M. Pereira Coelho, V. Scheurer, T. Tomei

Institute for Nuclear Research and Nuclear Energy, Bulgarian Academy of Sciences, Sofia,

Bulgaria
A. Aleksandrov, G. Antchev, P. Danev, R. Hadjiiska, P. Iaydjiev, M. Shopova, G. Sultanov

University of Sofia, Sofia, Bulgaria
A. Dimitrov, L. Litov, B. Pavlov, P. Petkov, A. Petrov

Instituto de Alta Investigación, Universidad de Tarapacá, Arica, Chile
S. Keshri, D.N. Laroze Navarrete, M. Meena, S. Thakur

Universidad Técnica Federico Santa María, Valparaiso, Chile
W. Brooks

Beihang University, Beijing, China
T. Cheng, L. Wang, L. Yuan

Department of Physics, Tsinghua University, Beijing, China
J. Gu, Z. Hu, Z. Liang, J. Liu, X. Wang, Y. Wang, H. Yang, S. Zhang, Y. Zhao

Institute of High Energy Physics, Beijing, China
N. Bi[8], G.M. Chen[8], H.S. Chen[8], M. Chen[8], Y. Chen, B. Hou[8], Q. Hou, F. Iemmi, C.H. Jiang, P.z. Lai, H. Liao, G. Liu, Z. Liu[8], S. Song[8], J. Tao, C. Wang[8], J. Wang, A. Zada[8], H. Zhang, J. Zhao

State Key Laboratory of Nuclear Physics and Technology, Peking University, Beijing, China
Y. Ban, A. Carvalho Antunes De Oliveira, S. Deng, X. Geng, B. Guo, Q. Guo, Z. He, C. Jiang, A. Levin, C. Li, L. Li, Q. Li, Y. Mao, S. Qian, S.J. Qian, X. Qin, C. Quaranta, X. Sun, D. Wang, J. Wang, T. Yang, M. Zhang, M. Zhang, Y. Zhao, C. Zhou

State Key Laboratory of Nuclear Physics and Technology, Institute of Quantum Matter, South China Normal University, Guangzhou, China, Guangzhou, China
X. Hua, S. Yang

Sun Yat-Sen University, Guangzhou, China
Z. You

University of Science and Technology of China, Hefei, China
N. Lu

Nanjing Normal University, Nanjing, China
G. Bauer[9,10], L. Chen, Z. Cui[10], B. Li[11], H. Wang, K. Yi[12], J. Zhang, F. Zhu

Institute of Frontier and Interdisciplinary Science, Shandong University, Qingdao, China
C. Li

Institute of Modern Physics and Key Laboratory of Nuclear Physics and Ion-beam Application (MOE) - Fudan University, Shanghai, China
Y. Li, Z. Wang, Y. Zhou[13]

Zhejiang University - Department of Physics, Zhejiang, China
Z. Lin, C. Lu, M. Xiao[14]

Universidad de Los Andes, Bogota, Colombia
C. Avila, A. Cabrera, C. Florez, J.A. Reyes Vega

Universidad de Antioquia, Medellin, Colombia

C. Rendón, M. Rodriguez, A.A. Ruales Barbosa, J.D. Ruiz Alvarez

University of Split, Faculty of Electrical Engineering, Mechanical Engineering and Naval Architecture, Split, Croatia
N. Godinovic, D. Lelas, I. Puljak, A. Sculac

University of Split, Faculty of Science, Split, Croatia
M. Kovac, A. Petkovic, T. Sculac

Institute Rudjer Boskovic, Zagreb, Croatia
P. Bargassa, V. Brigljevic, D. Ferencek, K. Jakovcic, A. Starodumov, T. Susa

University of Cyprus, Nicosia, Cyprus
A. Attikis, S. Konstantinou, C. Leonidou, L. Paizanos, F. Ptochos, P.A. Razis, H. Saka, A. Stepennov

Charles University, Prague, Czech Republic
M. Finger, M. Finger Jr., A. Kveton

Escuela Politecnica Nacional, Quito, Ecuador
E. Acurio

Universidad San Francisco de Quito, Quito, Ecuador
E. Carrera Jarrin

Academy of Scientific Research and Technology of the Arab Republic of Egypt, Egyptian Network of High Energy Physics, Cairo, Egypt
B. El-mahdy[15], S. Khalil[16], E. Salama[17,18]

Center for High Energy Physics (CHEP-FU), Fayoum University, El-Fayoum, Egypt
A. Hussein, M. Mahmoud, H. Mohammed, M.A.A. Muhammad

National Institute of Chemical Physics and Biophysics, Tallinn, Estonia
K. Jaffel, M. Kadastik, T. Lange, C. Nielsen, J. Pata, M. Raidal, N. Seeba, L. Tani

Department of Physics, University of Helsinki, Helsinki, Finland
E. Brücken, A. Milieva, K. Osterberg, M. Voutilainen

Helsinki Institute of Physics, Helsinki, Finland
F.I. Garcia Fuentes, T. Hilden, P. Inkaew, K.T.S. Kallonen, R. Kumar Verma, T. Lampén, K. Lassila-Perini, B. Lehtela, S. Lehti, T. Lindén, N.R. Mancilla Xinto, M. Myllymäki, M.m. Rantanen, S. Saariokari, N.T. Toikka, J. Tuominiemi, E. Veikkola

Lappeenranta-Lahti University of Technology, Lappeenranta, Finland
N. Bin Norjoharuddeen, H. Kirschenmann, P.R. Luukka, H. Petrow

IRFU, CEA, Université Paris-Saclay, Gif-sur-Yvette, France
M. Besancon, F. Couderc, M. Dejardin, D. Denegri, P. Devouge, J.L. Faure, F. Ferri, P. Gaigne, S. Ganjour, P. Gras, F. Guilloux, G. Hamel de Monchenault, M. Kumar, V. Lohezic, Y. Maidannyk, J. Malcles, F. Orlandi, L. Portales, S. Ronchi, M.Ö. Sahin, P. Simkina, M. Titov, M. Tornago

Laboratoire Leprince-Ringuet, CNRS/IN2P3, Ecole Polytechnique, Institut Polytechnique de Paris, Palaiseau, France
R. Amella Ranz, F. Beaudette, K. Biriukov, G. Boldrini, P. Busson, C. Charlot, M. Chiusi, T.D. Cuisset, O. Davignon, A. De Wit, T. Debnath, I.T. Ehle,

S. Ghosh, A. Gilbert, R. Granier de Cassagnac, M. Manoni, M. Nguyen, S. Obraztsov, C. Ochando, L.m. Rabour, R. Salerno, J.B. Sauvan, Y. Sirois, G. Sokmen, Y. Song, L. Urda Gómez, B. Voirin, A. Zabi, A. Zghiche

Institut Pluridisciplinaire Hubert Curien (IPHC), Université de Strasbourg, CNRS/IN2P3, Strasbourg, France
J.L. Agram[19], J. Andrea, D. Bloch, E.C. Chabert, C. Collard, G. Coulon, C. Eschenlauer, S. Falke, U. Goerlach, A.C. Le Bihan, G. Saha, A. Savoy-Navarro[20], P. Vaucelle

Centre de Calcul de l'Institut National de Physique Nucleaire et de Physique des Particules, CNRS/IN2P3, Villeurbanne, France
A. Di Florio, G. Mauceri, B. Orzari

Institut de Physique des 2 Infinis de Lyon (IP2I), Villeurbanne, France
D. Amram, S. Beauceron, B. Blancon, G. Boudoul, N. Chanon, D. Contardo, J. Daniel, P. Depasse, H. El Mamouni, J. Fay, E. Fillaudeau, S. Gascon, M. Gouzevitch, C. Greenberg, B. Ille, E. Jourd'Huy, M. Lethuillier, K. Long, B. Massoteau, L. Mirabito, A. Purohit, M. Vander Donckt, C. Verollet

Georgian Technical University, Tbilisi, Georgia
D. Chokheli, I. Lomidze, Z. Tsamalaidze[21]

RWTH Aachen University, I. Physikalisches Institut, Aachen, Germany
K.F. Adamowicz, V. Botta, S. Consuegra Rodríguez, L. Feld, K. Klein, M. Lipinski, P. Nattland, V. Oppenländer, A. Pauls, D. Pérez Adán

RWTH Aachen University, III. Physikalisches Institut A, Aachen, Germany
C. Daumann, S. Diekmann, E. Ehlert, N. Eich, D. Eliseev, F. Engelke, J. Erdmann, M. Erdmann, M.Z. Farkas, B. Fischer, T. Hebbeker, K. Hoepfner, A. Jung, N. Kumar, M.y. Lee, F. Mausolf, M. Merschmeyer, A. Meyer, A. Pozdnyakov, W. Redjeb, H. Reithler, U. Sarkar, V. Sarkisovi, A. Schmidt, J.G. Schulz, C. Seth, A. Sharma, J.L. Spah, V. Vaulin, U. Willemsen, S. Zaleski, F.P. Zinn

RWTH Aachen University, III. Physikalisches Institut B, Aachen, Germany
M.R. Beckers, G. Flügge, N. Hoeflich, T. Kress, A. Nowack, O. Pooth, A. Stahl

Deutsches Elektronen-Synchrotron, Hamburg, Germany
A. Abel, A. Akhil, M. Aldaya Martin, J. Alimena, Y. An, I. Andreev, J. Bach, S. Baxter, H. Becerril Gonzalez, O. Behnke, F. Blekman[22], K. Borras[23], A. Campbell, S. Chatterjee, L.X. Coll Saravia, G. Eckerlin, D. Eckstein, E. Gallo[22], A. Geiser, M. Guthoff, A. Hinzmann, U. Husemann, M. Kasemann, C. Kleinwort, R. Kogler, M. Komm, D. Krücker, F. Labe, W. Lange, D. Leyva Pernia, J.h. Li, K.y. Lin, K. Lipka[24], W. Lohmann[25], J. Malvaso, R. Mankel, I.A. Melzer-Pellmann, M. Mendizabal Morentin, A.B. Meyer, G. Milella, K. Moral Figueroa, A. Mussgiller, L.P. Nair, J. Niedziela, A. Nürnberg, J. Park, E. Ranken, A. Raspereza, D. Rastorguev, L. Rygaard, M. Scham[26,23], S. Schnake[23], C. Schwanenberger[22], D. Schwarz, P. Schütze, D. Selivanova, K. Sharko, M. Shchedrolosiev, A. Sritharan, D. Stafford, M. Torkian, S. Vashishtha, A. Ventura Barroso, R. Walsh, D. Wang, Q. Wang, K. Wichmann, L. Wiens[23], C. Wissing, Y. Yang, S. Zakharov, A. Zimermmane Castro Santos

University of Hamburg, Hamburg, Germany
A.R. Alves Andrade, M. Antonello, S. Bollweg, M. Bonanomi, L. Ebeling,

K. El Morabit, Y. Fischer, M. Frahm, P.P. Gadow, E. Garutti, A. Grohsjean, A.A. Guvenli, J. Haller, D. Hundhausen, M. Jalalvandi, G. Kasieczka, P. Keicher, R. Klanner, W. Korcari, T. Kramer, C.c. Kuo, J. Lange, A. Lobanov, J. Matthiesen, L. Moureaux, K. Nikolopoulos, K.J. Pena Rodriguez, N. Prouvost, B. Raciti, M. Rieger, D. Savoiu, P. Schleper, M. Schröder, J. Schwandt, M. Sommerhalder, H. Stadie, G. Steinbrück, T. von Schwartz, R. Ward, B. Wiederspan, M. Wolf, C. Yede

Institut für Experimentelle Teilchenphysik, Karlsruhe, Germany
J. Ahäuser, A. Brusamolino, E. Butz, Y.M. Chen, T. Chwalek, A. Dierlamm, G.G. Dincer, U. Elicabuk, N. Faltermann, M. Giffels, A. Gottmann, F. Hartmann[27], F. Hummer, J. Kieseler, M. Klute, H.A. Krause, R. Kunnilan Muhammed Rafeek, O. Lavoryk, J.M. Lawhorn, S. Maier, N. Meenamthuruthil Radhakrishnan, T. Mehner, M. Molch, A.A. Monsch, M. Mormile, T. Müller, E. Pfeffer, M. Presilla, G. Quast, K. Rabbertz, B. Regnery, R. Schmieder, T. Selezneva, N. Shadskiy, L. Sowa, L. Stockmeier, M. Toms, B. Topko, N. Trevisani, C. Verstege, T. Voigtländer, R.F. Von Cube, J. Von Den Driesch, C. Winter, R. Wolf, W.D. Zeuner, X. Zuo

Institute of Nuclear and Particle Physics (INPP), NCSR Demokritos, Aghia Paraskevi, Greece
G. Anagnostou, G. Daskalakis, A. Kyriakis

National and Kapodistrian University of Athens, Athens, Greece
P. Iosifidou, P. Katris, M. Kotsarini, G. Melachroinos, Z. Painesis, N. Plastiras, N. Saoulidou, K. Theofilatos, E. Tzovara, K. Vellidis, I. Zisopoulos

National Technical University of Athens, Athens, Greece
T. Chatzistavrou, G. Karapostoli, K. Kousouris, K. Paschos, L.P. Rouseliotaki, E. Siamarkou, A. Taxeidi, G. Tsipolitis

University of Ioánnina, Ioánnina, Greece
I. Evangelou, C. Foudas, P. Katsoulis, P. Kokkas, P.G. Kosmoglou Kioseoglou, N. Manthos, I. Papadopoulos, J. Strologas

Department of Physics, School of Sciences Democritus, University of Thrace, Kavala, Greece
E. Tziaferi

HUN-REN Wigner Research Centre for Physics, Budapest, Hungary
C. Hajdu, D. Horvath[28,29], Á. Kadlecsik, C. Lee, K. Márton, A.J. Rádl[30], F. Sikler, V. Veszpremi

MTA-ELTE Lendület CMS Particle and Nuclear Physics Group, Eötvös Loránd University, Budapest, Hungary
G. Balint, M. Csanad, K. Farkas, A. Fehérkuti[31], M.M.A. Gadallah[32], M. León Coello, G. Pasztor, G.I. Veres

Faculty of Informatics, University of Debrecen, Debrecen, Hungary, Debrecen, Hungary
B. Ujvari, G. Zilizi

HUN-REN ATOMKI - Institute of Nuclear Research, Debrecen, Hungary
G. Bencze, S. Czellar, J. Molnar, Z. Szillasi

Karoly Robert Campus, MATE Institute of Technology, Gyongyos, Hungary
T.F. Csorgo[31], F. Nemes[31], T. Novak, I. Szanyi[33]

Indian Institute of Science (IISC), Bangalore, India
J.R. Komaragiri

Indian Institute of Technology Bhubaneswar, Bhubaneswar, India
S. Bahinipati, R. Raturi

Panjab University, Chandigarh, India
S. Bansal, V. Bhatnagar, B. Chauhan, S. Chauhan, N. Dhingra[34], A. Kaur, H. Kaur, S. Kumar, T. Sheokand, A. Singla, K. Verma

University of Delhi, Delhi, India
A. Bhardwaj, A. Chhetri, B.C. Choudhary, A. Kumar, A. Kumar, M. Naimuddin, S. Phor, C. Prakash, K. Ranjan, M.K. Saini

Indian Institute of Technology Mandi (IIT-Mandi), Himachal Pradesh, India
M. Kumari, P. Palni, S. Rana, A. Rathore, A. Sarkar

University of Hyderabad, Hyderabad, India
S. Acharya[35], B. Gomber, S.K. Satapathy

Indian Institute of Technology Kanpur, Kanpur, India
S. Mukherjee

Saha Institute of Nuclear Physics, HBNI, Kolkata, India
S. Bhattacharya, S. Das Gupta, S. Dutta, S. Dutta, S. Sarkar

Indian Institute of Technology Madras, Madras, India
M.M. Ameen, P.K. Behera, S. Chatterjee, G. Dash, A. Dattamunsi, P. Jana, P. Kalbhor, S. Kamble, P.R. Pujahari, A.K. Sikdar, R.K. Singh, P. Verma, S. Verma, A. Vijay

Indian lnstitute of Science Education and Research Mohali, Mohali, India
A. Chauhan, S. Nayak, H. Rajpoot, B.K. Sirasva

Tata Institute of Fundamental Research-A, Mumbai, India
L. Bhatt, S. Dugad, T. Mishra, G.B. Mohanty, M. Shelake, P. Suryadevara

Tata Institute of Fundamental Research-B, Mumbai, India
A. Bala, S. Banerjee, S. Barman[36], R.M. Chatterjee, J. Chhikara, M. Guchait, S. Jain, A. Jaiswal, S. Kumar, M. Maity[36], G. Majumder, K. Mazumdar, R. Pramanik, R. Saxena, P. Sharma, A. Thachayath

National Institute of Science Education and Research, Jatni, Khorda, Odisha 752050, India Homi Bhabha National Institute, Training School Complex, Anushakti Nagar, Mumbai 400094, India, Odisha, India
R. Kumar Agrawal, D. Maity[37], P. Mal, K. Naskar[37], A. Nayak[37], K. Pal, P. Sadangi, S. Shuchi, S.K. Swain, S. Varghese[37], D. Vats[37]

Indian Institute of Science Education and Research (IISER), Pune, India
S. Dube, P. Hazarika, B. Kansal, A. Laha, R. Sharma, S. Sharma, K.Y. Vaish

Indian Institute of Technology Hyderabad, Telangana, India
C. Agrawal, B. Babu, S. Ghosh

Isfahan University of Technology, Isfahan, Iran
H. Bakhshiansohi[38], A. Jafari[39], V. Sedighzadeh Dalavi, M. Zeinali[40]

Institute for Research in Fundamental Sciences (IPM), Tehran, Iran
S. Bashiri, S. Chenarani[41], S.M. Etesami, Y. Hosseini, M. Khakzad, E. Khazaie, M. Mohammadi Najafabadi, M. Nourbakhsh, S. Tizchang[42]

University College Dublin, Dublin, Ireland
M. Felcini, M. Grunewald

INFN Sezione di Bari[a], Università di Bari[b], Politecnico di Bari[c], Bari, Italy
M. Abbrescia[a,b], M. Buonsante[a,b], A. Colaleo[a,b], D. Creanza[a,c], N. De Filippis[a,c], M. De Palma[a,b], W. Elmetenawee[a,b,43], N. Ferrara[a,c], L. Fiore[a], L. Generoso[a,b], L. Longo[a], M. Louka[a,b], G. Maggi[a,c], M. Maggi[a], S. My[a,b], F. Nenna[a,b], S. Nuzzo[a,b], A. Pellecchia[a,b], A. Pompili[a,b], F.M. Procacci[a,b], G. Pugliese[a,c], R. Radogna[a,b], D. Ramos[a], A. Ranieri[a], L. Silvestris[a], F.M. Simone[a,b], A. Stamerra[a,b], Ü. Sözbilir[a,44], D. Troiano[a,b], R. Venditti[a,b], P. Verwilligen[a], A. Zaza[a,b]

INFN Sezione di Bologna[a], Università di Bologna[b], Bologna, Italy
G. Abbiendi[a], S. Balducci[a,b], C. Battilana[a,b], D. Bonacorsi[a,b], P. Capiluppi[a,b], F.R. Cavallo[a], M. Cruciani[a,b], M. Cuffiani[a,b], G.M. Dallavalle[a], T. Diotalevi[a,b], F. Fabbri[a], A. Fanfani[a,b], R. Farinelli[a], D. Fasanella[a], L. Ferragina[a,b], C. Grandi[a], L. Guiducci[a,b], M. Lorusso[a,b], L. Lunerti[a], S. Marcellini[a], G. Masetti[a], F. Navarria[a,b], G. Paggi[a,b], A. Perrotta[a], A. Rossi[a,b], S. Rossi Tisbeni[a,b], T. Rovelli[a,b]

INFN Sezione di Catania[a], Università di Catania[b], Catania, Italy
S. Costa[a,b,45], A. Di Mattia[a], A. Lapertosa[a], R. Potenza[a,b], A. Tricomi[a,b,45]

INFN Sezione di Firenze[a], Università di Firenze[b], Firenze, Italy
J. Altork[a,b], G. Barbagli[a], G. Bardelli[a], A. Calandri[a,b], B. Camaiani[a,b], A. Cassese[a], R. Ceccarelli[a], V. Ciulli[a,b], C. Civinini[a], R. D'Alessandro[a,b], L. Damenti[a,b], E. Focardi[a,b], T. Kello[a], G. Latino[a,b], P. Lenzi[a,b], M. Lizzo[a], M. Meschini[a], S. Paoletti[a], A. Papanastassiou[a,b], G. Sguazzoni[a], L. Viliani[a]

INFN Laboratori Nazionali di Frascati, Frascati, Italy
L. Benussi, S. Colafranceschi[46], S. Meola[47], D. Piccolo

INFN Sezione di Genova[a], Università di Genova[b], Genova, Italy
M. Alves Gallo Pereira[a], F. Ferro[a], E. Robutti[a], S. Tosi[a,b]

INFN Sezione di Milano-Bicocca[a], Università di Milano-Bicocca, Milano[b], Milano-Bicocca, Italy
A. Benaglia[a], F. Brivio[a], V. Camagni[a,b], F. Cetorelli[a,b], F. De Guio[a,b], M.E. Dinardo[a,b], P. Dini[a], S. Gennai[a], R. Gerosa[a,b], A. Ghezzi[a,b], P. Govoni[a,b], L. Guzzi[a], G. Lavizzari[a,b], M.T. Lucchini[a,b], M. Malberti[a], S. Malvezzi[a], A. Massironi[a], L. Moroni[a], M. Paganoni[a,b], S. Palluotto[a,b], D. Pedrini[a], A. Perego[a,b], T. Tabarelli de Fatis[a,b]

INFN Sezione di Napoli[a], Università di Napoli 'Federico II'[b], Università della Basilicata (Potenza)[c], Scuola Superiore Meridionale (SSM)[d], Napoli, Italy
S. Buontempo[a], F. Confortini[a,b], C. Di Fraia[a,b], F. Fabozzi[a,c], L. Favilla[a,d], A.O.M. Iorio[a,b], L. Lista[a,b,48], P. Paolucci[a,27], B. Rossi[a]

INFN Sezione di Padova[a], Università di Padova[b], Universita degli Studi di Cagliari[c], Padova, Italy

P. Azzi[a], N. Bacchetta[a,49], D. Bisello[a,b], L. Borella[a], P. Bortignon[a,c], G. Bortolato[a,b], A.C.M. Bulla[a,c], R. Carlin[a,b], P. Checchia[a], T. Dorigo[a,50], F. Gasparini[a,b], U. Gasparini[a,b], S. Giorgetti[a], P. Grutta[a], N. Lai[a], E. Lusiani[a], M. Margoni[a,b], A.T. Meneguzzo[a,b], M. Missiroli[a], J. Pazzini[a,b], F. Primavera[a,b], P. Ronchese[a,b], R. Rossin[a,b], F. Simonetto[a,b], M. Toffano[a], M. Tosi[a,b], A. Triossi[a,b], S. Ventura[a], M. Zanetti[a,b], P. Zotto[a,b], A. Zucchetta[a,b], G. Zumerle[a,b]

INFN Sezione di Pavia[a], Università di Pavia[b], Pavia, Italy
S. A. AbuZeid[a,18], C. Aimè[a], A. Braghieri[a], M. Brunoldi[a,b], P. Montagna[a,b], M. Pelliccioni[a,b], V. Re[a], C. Riccardi[a,b], P. Salvini[a], I. Vai[a,b], P. Vitulo[a,b]

INFN Sezione di Perugia[a], Università di Perugia[b], Perugia, Italy
S. Ajmal[a,b], M.E. Ascioti[a,b], G.M. Bilei[a], W.D. Buitrago Ceballos[a,b], C. Carrivale[a,b], D. Ciangottini[a,b], L. Della Penna[a,b], L. Fanò[a,b], V. Mariani[a,b], M. Menichelli[a], F. Moscatelli[a,51], F. Napolitano[a], A. Rossi[a,b], A. Santocchia[a,b], D. Spiga[a], T. Tedeschi[a,b]

INFN Sezione di Pisa[a], Università di Pisa[b], Scuola Normale Superiore di Pisa[c], Università di Siena[d], Pisa, Italy
C.A. Alexe[a,c], P. Asenov[a,b], P. Azzurri[a], G. Bagliesi[a], L. Bianchini[a,b], T. Boccali[a], E. Bossini[a], D. Bruschini[a,c], R. Castaldi[a], F. Cattafesta[a,c], M.A. Ciocci[a,d], M. Cipriani[a,b], R. Dell'Orso[a], S. Dhani[a,d], S. Donato[a,b], A. Feliziani[a,d], R. Forti[a,b], A. Giassi[a], F. Ligabue[a,c], A.C. Marini[a,b], A. Messineo[a,b], S. Mishra[a], V.K. Muraleedharan Nair Bindhu[a,b], S. Nandan[a], F. Palla[a], M. Riggirello[a,c], A. Rizzi[a,b], G. Rolandi[a,c], A. Scribano[a], P. Solanki[a,b], P. Spagnolo[a], F. Tenchini[a,b], R. Tenchini[a], G. Tonelli[a,b], N. Turini[a,d], F. Vaselli[a,c], A. Venturi[a], P.G. Verdini[a]

INFN Sezione di Roma[a], Sapienza Università di Roma[b], Roma, Italy
P. Akrap[a,b], C. Basile[a,b], S.C. Behera[a], F. Cavallari[a], L. Cunqueiro Mendez[a,b], F. De Riggi[a,b], D. Del Re[a,b], M. Del Vecchio[a,b], E. Di Marco[a], M. Diemoz[a], F. Errico[a], L. Frosina[a,b], R. Gargiulo[a,b], B. Harikrishnan[a,b], F. Lombardi[a,b], L. Martikainen[a,b], G. Organtini[a,b], N. Palmeri[a,b], R. Paramatti[a,b], T. Pauletto[a,b], S. Rahatlou[a,b], C. Rovelli[a], F. Santanastasio[a,b], L. Soffi[a], V. Vladimirov[a,b]

INFN Sezione di Torino[a], Università di Torino[b], Università del Piemonte Orientale (Novara)[c], Torino, Italy
N. Amapane[a,b], R. Arcidiacono[a,c], S. Argiro[a,b], M. Arneodo[a,c], N. Bartosik[a,c], F. Bashir[a,b], R. Bellan[a,b], A. Bellora[a,b], C. Biino[a], C. Borca[a,b], N. Cartiglia[a], M. Costa[a,b], R. Covarelli[a,b], N. Demaria[a], E. Ferrando[a,b], L. Finco[a], M. Grippo[a,b], B. Kiani[a,b], L. Lanteri[a,b], F. Luongo[a,b], M. Marchisio Caprioglio[a,b], C. Mariotti[a,52], S. Maselli[a], A. Mecca[a,b], L. Menzio[a,b], P. Meridiani[a], E. Migliore[a,b], M. Monteno[a], M.M. Obertino[a,b], G. Ortona[a], L. Pacher[a,b], N. Pastrone[a], M. Ruspa[a,c], F. Siviero[a,b], V. Sola[a,b], A. Solano[a,b], A. Staiano[a], C. Tarricone[a,b], D. Trocino[a], G. Umoret[a,b], E. Vlasov[b], R. White[a,b]

INFN Sezione di Trieste[a], Università di Trieste[b], Trieste, Italy
J. Babbar[a,b,53], S. Belforte[a], V. Candelise[a,b], M. Casarsa[a], F. Cossutti[a], K. De Leo[a], G. Della Ricca[a,b], R. Delli Gatti[a,b], C. Giraldin[a,b]

Kyungpook National University, Daegu, Korea
S. Dogra, J. Hong, J. Kim, J. Kim, T. Kim, D. Lee, H. Lee, J. Lee, S.W. Lee, C.S. Moon, Y.D. Oh, S. Sekmen, B. Tae, Y.C. Yang

Department of Mathematics and Physics - Gangneung-Wonju National University, Gangneung, Korea
M.S. Kim

Chonnam National University, Institute for Universe and Elementary Particles, Kwangju, Korea
G. Bak, P. Gwak, H. Kim, H. Lee, S. Lee, D.H. Moon, J. Seo

Department of Physics, Chung-Ang University, Seoul, Korea
K. Lee, Y. Lee

Hanyang University, Seoul, Korea
E. Asilar, F. Carnevali, J. Choi[54], T.J. Kim, Y. Ryou, J. Song, T. Yang

Korea University, Seoul, Korea
S. Ha, B.S. Hong, J. Kim, K. Lee, K. Lee, S. Lee, J. Padmanaban, B.A.N. Putra, J. Yoo

Kyung Hee University, Department of Physics, Seoul, Korea
J. Goh, J. Shin, S. Yang

Sejong University, Seoul, Korea
L. Kalipoliti, Y. Kang, H. Kim, Y. Kim, B. Ko, S. Lee

Seoul National University, Seoul, Korea
J.H. Bhyun, J. Choi, J. Choi, W. Jun, H. Kim, J. Kim, J. Kim, T. Kim, Y. Kim, Y.W. Kim, S. Ko, H. Lee, J. Lee, J. Lee, B.H. Oh, J. Shin, U. Yang, I. Yoon

University of Seoul, Seoul, Korea
S. Calzaferri, W. Heo, W. Jang, D. Kim, S. Kim, J.S.H. Lee, Y. Roh, I. J. Watson

Yonsei University, Department of Physics, Seoul, Korea
G. Cho, Y. Eo, K. Hwang, H. Jang, B. Kim, D. Kim, S. Kim, G. Mocellin, H.D. Yoo

Sungkyunkwan University, Suwon, Korea
Y. Lee, I. Yu

College of Engineering and Technology, American University of the Middle East (AUM), Dasman, Kuwait
T. Beyrouthy, Y. Gharbia

Kuwait University - College of Science - Department of Physics, Safat, Kuwait
F. Alazemi

Riga Technical University, Riga, Latvia
K. Dreimanis, O.M. Eberlins, A. Gaile, J.K. Heikkilä, M. Klevs, C. Munoz Diaz, D. Osite, G. Pikurs, R. Plese, A. Potrebko, M. Seidel, D. Sidiropoulos Kontos

University of Latvia (LU), Riga, Latvia
N.R. Strautnieks

Vilnius University, Vilnius, Lithuania
M. Ambrozas, A. Juodagalvis, S. Nargelas, S. Nayak, G. Tamulaitis

National Centre for Particle Physics, Universiti Malaya, Kuala Lumpur, Malaysia
I. Yusuff[55], Z. Zolkapli

University of Sonora (UNISON), Hermosillo, Mexico

J.P. Barajas Ibarria, J.F. Benitez, A. Castaneda Hernandez, A. Cota Rodriguez, L.E. Cuevas Picos, H.A. Encinas Acosta, L.G. Gallegos Maríñez, J.A. Murillo Quijada, L. Valencia Palomo

Centro de Investigacion y de Estudios Avanzados del IPN, Mexico City, Mexico
G. Ayala, H. Castilla-Valdez, H. Crotte Ledesma, R. Lopez-Fernandez, J. Mejia Guisao, R. Reyes-Almanza, A. Sánchez Hernández

Universidad Iberoamericana, Mexico City, Mexico
C. Oropeza Barrera, D.L. Ramirez Guadarrama, M. Ramírez García

Benemerita Universidad Autonoma de Puebla, Puebla, Mexico
I. Bautista, F.E. Neri Huerta, I. Pedraza, H.A. Salazar Ibarguen, C. Uribe Estrada

University of Montenegro, Podgorica, Montenegro
I. Bubanja, J. Mijuskovic, N. Raicevic

National Centre for Physics, Quaid-I-Azam University, Islamabad, Pakistan
A. Ahmad, M.I. Asghar, A. Awais, M.I.M. Awan, W.A. Khan, I. Sohail

AGH University of Krakow, Krakow, Poland
V. Avati, L. Forthomme, L. Grzanka, M. Malawski, K. Piotrzkowski

National Centre for Nuclear Research, Swierk, Poland
H. Awedikian, M. Bluj, M. Ghimiray, M. Górski, M. Kazana, M. Szleper, P. Zalewski

Institute of Experimental Physics, Faculty of Physics, University of Warsaw, Warsaw, Poland
K. Bunkowski, K. Doroba, A. Kalinowski, M. Konecki, J. Krolikowski, W. Matyszkiewicz, A. Muhammad, S. Slawinski

Warsaw University of Technology, Warsaw, Poland
P. Fokow, K. Pozniak, W. Zabolotny

Laboratório de Instrumentação e Física Experimental de Partículas, Lisboa, Portugal
M. Araujo, C. Beirão Da Cruz E Silva, A. Boletti, M. Bozzo, T. Camporesi[52,56], G. Da Molin, M. Gallinaro, R. Guitton, J. Hollar, H. Legoinha, N. Leonardo[57], G.B. Marozzo, A. Petrilli, M. Pisano, J. Seixas, J. Varela, J.W. Wulff

Faculty of Physics, University of Belgrade, Belgrade, Serbia
P. Adzic, L. Markovic, P. Milenovic, V. Milosevic

Vinca Institute of Nuclear Science, Belgrade, Serbia
D. Devetak, M. Dordevic, J. Milosevic, L. Nadderd, V. Rekovic, M. Stojanovic

Centro de Investigaciones Energéticas Medioambientales y Tecnológicas (CIEMAT), Madrid, Spain
M. Alcalde Martinez, J. Alcaraz Maestre, J.A. Brochero Cifuentes, M. Cepeda, M. Cerrada, N. Colino, B. De La Cruz, A. Escalante Del Valle, C. Fernandez Bedoya, D. Fernández Del Val, J.P. Fernández Ramos, J. Flix, M.C. Fouz, M. Gonzalez Hernandez, O. Gonzalez Lopez, S. Goy Lopez, J.M. Hernandez, M.I. Josa, J. Llorente Merino, O. Manzanilla, C. Martin Perez, E. Martin Viscasillas, D. Moran, C.M. Morcillo Perez, Á. Navarro Tobar, J. Puerta Pelayo, A.M. Pérez-Calero Yzquierdo, I. Redondo, D.D. Redondo Ferrero, J. Vazquez Escobar

Universidad Autónoma de Madrid, Madrid, Spain

J.F. de Trocóniz

Universidad de Oviedo, Instituto Universitario de Ciencias y Tecnologías Espaciales de Asturias (ICTEA), Oviedo, Spain
E. Aller Gutierrez, B. Alvarez Gonzalez, J. Ayllon Torresano, A. Cardini, J. Cuevas, J. Del Riego Badas, D. Estrada Acevedo, J. Fernandez Menendez, S. Folgueras, I. Gonzalez Caballero, P. Leguina, M. Obeso Menendez, E. Palencia Cortezon, J. Prado Pico, S. Sanchez Cruz, A. Soto Rodríguez, P. Vischia

Instituto de Física de Cantabria (IFCA), CSIC-Universidad de Cantabria, Santander, Spain
S. Blanco Fernández, I.J. Cabrillo, A. Calderon, M. Caserta, J. Duarte Campderros, M. Fernandez, G. Gomez, C. Lasaosa García, R. Lopez Ruiz, C. Martinez Rivero, P. Martinez Ruiz del Arbol, F. Matorras, P. Matorras Cuevas, E. Navarrete Ramos, J. Piedra Gomez, C. Quintana San Emeterio, V. Rodriguez, L. Scodellaro, I. Vila, R. Vilar Cortabitarte, J.M. Vizan Garcia

University of Colombo, Colombo, Sri Lanka
B. Kailasapathy[58]

University of Ruhuna, Department of Physics, Matara, Sri Lanka
W.G. Dharmaratna[59], N. Perera

CERN, European Organization for Nuclear Research, Geneva, Switzerland
D. Abbaneo, C. Amendola, R. Ardino, E. Auffray, J. Baechler, D. Barney, J. Bendavid, I. Bestintzanos, M. Bianco, A. Bocci, L. Borgonovi, C. Botta, A. Bragagnolo, C.E. Brown, C. Caillol, G. Cerminara, P. Connor, K. Cormier, D. D'Enterria, A. Dabrowski, P. Das, A. David Tinoco Mendes, A. De Roeck, M.M. Defranchis, M. Deile, M. Dobson, P.J. Fernández Manteca, E. Fialova, B.A. Fontana Santos Alves, E. Fontanesi, W. Funk, A. Gaddi, S. Giani, D. Gigi, K. Gill, F. Glege, M. Glowacki, A. Gruber, J. Hegeman, R. Hofsaess, B. Huber, T. James, P. Janot, L. Jeppe, O. Kaluzinska, O. Karacheban[25], G. Karathanasis, S. Laurila, P. Lecoq, E. Leutgeb, J. León Holgado, C. Lourenco, A.m. Lyon, M. Magherini, L. Malgeri, E. Manca, M. Mannelli, F. Meijers, J.A. Merlin, S. Mersi, E. Meschi, M. Migliorini, F. Monti, F. Moortgat, M.C. Muehlnikel, M. Mulders, M. Musich, I. Neutelings, S. Orfanelli, F. Pantaleo, M. Pari, F. Pereira Carneiro, G. Petrucciani, A. Pfeiffer, M. Pierini, M. Pitt, H. Qu, A. Reimers, B. Ribeiro Lopes, F. Riti, P. Rosado, M. Rovere, H. Sakulin, R. Salvatico, S. Scarfi, S.F. Schaefer, M. Selvaggi, P. Silva, P. Sphicas[60], A.G. Stahl Leiton, A. Steen, S. Summers, G. Terragni, D. Treille, P. Tropea, E. Vernazza, M. Vojinovic, J. Wanczyk[61], S. Wuchterl, M. Zarucki, P. Zehetner, P. Zejdl, G. Zevi Della Porta

PSI Center for Neutron and Muon Sciences, Villigen, Switzerland
L. Caminada[62], W. Erdmann, R. Horisberger, Q. Ingram, H.C. Kaestli, D. Kotlinski, C. Lange, U. Langenegger, A. Nigamova, L. Noehte[62], L. Redard-Jacot[62], T. Rohe, A. Samalan

ETH Zurich - Institute for Particle Physics and Astrophysics (IPA), Zurich, Switzerland
T.K. Aarrestad, M. Backhaus, A. Belvedere, T. Bevilacqua[62], G. Bonomelli, C. Cazzaniga, K. Datta, P. De Bryas Dexmiers D'Archiacchiac[61], A. De Cosa, G. Dissertori, M. Dittmar, M. Donegà, F. Glessgen, C. Grab, T.G. Harte, N. Härringer, B. Kaynak, M. Koppel, W. Lustermann, M. Malucchi, R.A. Manzoni, L. Marchese, F. Nessi-Tedaldi, F. Pauss, A.A. Petre, J. Prendi, B. Ristic, S. Rohletter, P.M. Sander, R. Seidita, J. Steggemann[61], A. Tarabini, C.Z. Tee,

D. Valsecchi, P.H. Wagner, R. Wallny

Universität Zürich, Zurich, Switzerland
C. Amsler[63], F. Bilandzija, P. Bärtschi, M.F. Canelli, G. Celotto, Z. Ghafoor, T.A. Goldschmidt, V. Guglielmi, A. Jofrehei, B. Kilminster, T.H. Kwok, S. Leontsinis, V. Lukashenko, A. Macchiolo, F. Meng, J. Motta, P. Robmann, E. Shokr, F. Stäger, R. Tramontano, P. Viscone

Çukurova University, Adana, Türkiye
D. Agyel, F. Dolek, I. Dumanoglu[64], Y. Guler[65], E. Gurpinar Guler[65], A. Kayis Topaksu, G. Onengut, K. Ozdemir[66], B. Tali[67], U.G. Tok, E. Uslan

Hacettepe University, Ankara, Türkiye
S. Sen

Bogazici University, Istanbul, Türkiye
B. Akgun, I.O. Atakisi[68], E. Gulmez, M. Kaya[69], O. Kaya[70], M.A. Sarkisla[71], S. Tekten[72]

Istanbul Technical University, Istanbul, Türkiye
D. Boncukcu, A. Cakir, K. Cankocak[64,73], M. Gumustekin, A.D. Gungordu

Istanbul University, Istanbul, Türkiye
B. Hacisahinoglu, I. Hos[74], S. Ozkorucuklu, O. Potok, H. Sert, C. Simsek, C. Zorbilmez

Yildiz Technical University, Istanbul, Türkiye
S. Cerci, C. Dozen[75], E. Iren[76], B. Isildak, E. Simsek, D. Sunar Cerci, T. Yetkin[75]

National Central University, Chung-Li, Taiwan
D. Bhowmik, Y.h. Chou, C.M. Kuo, P.K. Rout, S. Taj, P.C. Tiwari[77]

National Taiwan University (NTU), Taipei, Taiwan
L. Ceard, K.F. Chen, Z.g. Chen, A. De Iorio, G.W.S. Hou, T.h. Hsu, Y.w. Kao, S. Karmakar, F. Khuzaimah, G. Kole, Y.y. Li, R.S. Lu, E. Paganis, X.f. Su, J. Thomas-Wilsker, L.s. Tsai, D. Tsionou, H.y. Wu, E. Yazgan

High Energy Physics Research Unit, Department of Physics, Faculty of Science, Chulalongkorn University, Bangkok, Thailand
C. Asawatangtrakuldee, N. Srimanobhas

Tunis El Manar University, Tunis, Tunisia
Y. Maghrbi

Institute for Scintillation Materials of National Academy of Science of Ukraine, Kharkiv, Ukraine
O. Dadazhanova, B. Grynyov

National Science Centre, Kharkiv Institute of Physics and Technology, Kharkiv, Ukraine
K. Klimenko, O. Kurov, L. Levchuk, S. Lukyanenko, A. Pristavka, D. Soroka

University of Bristol, Bristol, United Kingdom
J.J. Brooke, A. Bundock, F.J.J. Bury, E. Clement, D. Cussans, D. Dharmender, H. Flacher, J. Goldstein, H.F. Heath, M.l. Holmberg, A. Karakoulaki, L. Kreczko, S. Paramesvaran, L. Robertshaw, M.S. Sanjrani[38], J. Segal, V.J. Smith

Rutherford Appleton Laboratory, Didcot, United Kingdom

A. Ball, K.W. Bell, A. Belyaev[78], C. Brew, R.M. Brown, D.J. Cockerill, A. Elliot, K.V. Ellis, J. Gajownik, K. Harder, S. Harper, J. Linacre, K. Manolopoulos, M. Moallemi, D.M. Newbold, E. Olaiya, D. Petyt, T. Reis, A.R. Sahasransu, T. Schuh, C. Shepherd-Themistocleous, I.R. Tomalin, K.C. Whalen, T. Williams

Imperial College, London, United Kingdom
I. Andreou, S. Awan, R. Bainbridge, P. Bloch, O. Buchmuller, C.A. Carrillo Montoya, D. Colling, A. Cox, I. Das, P. Dauncey, G. Davies, M. Della Negra, S. Fayer, G. Fedi, G. Hall, H.R. Hoorani, A. Howard, G. Iles, C.R. Knight, P. Krueper, J. Langford, K.H. Law, L. Lyons, A.M. Magnan, B. Maier, S. Mallios, A. Mastronikolis, J. Nash[79], M. Pesaresi, P.B. Pradeep, E.V. Protopapa, B.C. Radburn-Smith, A. Richards, A. Rose, T.B. Runting, L. Russell, K. Savva, R. Schmitz, C. Seez, R. Shukla, A. Tapper, T. Travis, K. Uchida, G.P. Uttley, T. Virdee[27], N. Wardle, D. Winterbottom, J. Xiao

Brunel University, Uxbridge, United Kingdom
J. Cole, L. Juckett, A. Khan, P. Kyberd, I. Reid

The University of Alabama, Tuscaloosa, Alabama, USA
B. Bam, A. Buchot Perraguin, S. Campbell, R. Chudasama, S. Cooper, C. Crovella, G. Fidalgo, S.V. Gleyzer, R. Kaur, A. Khukhunaishvili, K. Matchev, E. Pearson, P. Rumerio[80], E. Usai, R. Yi

University of California, Davis, Davis, California, USA
S. Abbott, S. Baradia, B. Barton, R. Breedon, H. Cai, M. Calderon De La Barca Sanchez, E. Cannaert, M. Chertok, M. Citron, J. Conway, P.T. Cox, F. Eble, R. Erbacher, C. Fairchild, O. Kukral, S. Ostrom, I. Salazar Segovia, J.H. Steenis, J.S. Tafoya Vargas, W. Wei, S. Yoo

University of California, San Diego, La Jolla, California, USA
A. Aportela, A. Arora, J.G. Branson, S. Cittolin, B. D'Anzi, D. Diaz, J. Duarte, L. Giannini, Y. Gu, J. Guiang, V. Krutelyov, R. Lee, J. Letts, H. Li, R. Marroquin Solares, M. Masciovecchio, F. Mokhtar, S. Morovic, S. Mukherjee, M. Pieri, D. Primosch, M. Quinnan, V. Sharma, M. Tadel, E. Vourliotis, F. Würthwein, A. Yagil, Z. Zhao

University of California, Los Angeles, California, USA
K. Adamidis, H. Ancelin, M. Bachtis, D. Campos, R. Cousins, S. Crossley, G. Flores Avila, J. Hauser, M. Ignatenko, M.A. Iqbal, T. Lam, Y.f. Lo, A. Nunez Del Prado, D. Saltzberg, V. Valuev

California Institute of Technology, Pasadena, California, USA
A. Albert, S. Bhattacharya, A. Bornheim, O. Cerri, Z. Hao, L. Mori, H.B. Newman, G. Reales Gutiérrez, T. Sievert, P. Simmerling, E. Sledge, M. Spiropulu, C. Sun, J.R. Vlimant, R.A. Wynne, S. Xie, R.Y. Zhu

University of California, Riverside, Riverside, California, USA
R. Clare, J.W. Gary, G. Hanson

University of California, Santa Barbara - Department of Physics, Santa Barbara, California, USA
A. Barzdukas, L. Brennan, C. Campagnari, S. Carron Montero[81], K. Downham, C. Grieco, J.S. Guo, M.M. Hussain, D. Imani, J. Incandela, M.W.K. Lai, A.J. Li, P. Masterson, J.J.H. Ockenfuss, J. Richman, S.N. Santpur, D. Stuart, T.Á. Vámi,

X. Yan, D. Zhang

University of Colorado Boulder, Boulder, Colorado, USA
J.P. Cumalat, W.T. Ford, J. Fraticelli, A. Hart, M. Herrmann, S. Kwan, J. Pearkes, N. Schonbeck, K. Stenson, K. Ulmer, S.R. Wagner, N. Zipper, D. Zuolo

The Catholic University of America, Washington, DC, USA
R. Bartek, A. Dominguez, S. Raj, B. Sahu, A.E. Simsek, B. Singhal, S.S. Yu

University of Florida, Gainesville, Florida, USA
C. Aruta, P. Avery, D. Bourilkov, P. Chang, V. Cherepanov, M. Dittrich, R.D. Field, C. Huh, E. Koenig, M. Kolosova, J. Konigsberg, A. Korytov, G. Mitselmakher, K. Mohrman, A. Muthirakalayil Madhu, N. Rawal, S. Rosenzweig, Y. Takahashi, J. Wang

Florida Institute of Technology, Melbourne, Florida, USA
B. Alsufyani, S. Das, S. Demarest, L. Hasa, M. Hohlmann, M. Lavinsky, E. Yanes

Florida State University, Tallahassee, Florida, USA
T. Adams, A. Al Kadhim, D. Alam, A. Askew, S. Bower, R. Goff, R. Hashmi, A. Hassani, T. Kolberg, G. Martinez, M. Mazza, H. Prosper, P.R. Prova, R. Yohay

Fermi National Accelerator Laboratory, Batavia, Illinois, USA
M. Albrow, M. Alyari, O. Amram, G. Apollinari, A. Apresyan, L.A. Bauerdick, D. Berry, J. Berryhill, P.C. Bhat, K. Burkett, J.N. Butler, A. Canepa, G.B. Cerati, H. Cheung, F. Chlebana, C. Cosby, G. Cummings, I. Dutta, V.D. Elvira, J. Freeman, A. Gandrakota, Z. Gecse, L. Gray, D. Green, A. Grummer, S. Grünendahl, D. Guerrero, O. Gutsche, R.M. Harris, J. Hirschauer, V. Innocente, B. Jayatilaka, S. Jindariani, M. Johnson, R.S. Kim, S. Lammel, D. Lincoln, R. Lipton, T. Liu, K. Maeshima, D. Mason, P. McBride, P. Merkel, S. Mrenna, S. Nahn, J. Ngadiuba, D. Noonan, S. Norberg, V. Papadimitriou, N. Pastika, K. Pedro, C. Pena[82], C.E. Perez Lara, V. Perovic, F. Ravera, A. Reinsvold Hall[83], L. Ristori, M. Safdari, E. Sexton-Kennedy, E. Smith, N. Smith, A. Soha, L. Spiegel, S. Stoynev, J. Strait, L. Taylor, S. Tkaczyk, N.V. Tran, L. Uplegger, E.W. Vaandering, C. Wang, I. Zoi

University of Illinois Chicago, Chicago, Illinois, USA
M.R. Adams, N. Barnett, A. Baty, C. Bennett, N. Brandman-hughes, R. Cavanaugh, S.J. Das, R. Escobar Franco, O. Evdokimov, C.E. Gerber, H. Gupta, M. Hawksworth, A. Hingrajiya, D.J. Hofman, Z. Huang, J.h. Lee, C. Mills, S. Nanda, G. Nigmatkulov, B. Ozek, V. Pant, T. Phan, D. Pilipovic, R. Pradhan, E. Prifti, T. Roy, D. Shekar, N. Singh, F. Strug, A. Thielen, M. Tonjes, N. Varelas, M.A. Wadud, A. Wang, J. Yoo

Northwestern University, Evanston, Illinois, USA
S. Dittmer, K.A. Hahn, S. King, D. Li, M. Mcginnis, Y. Miao, D.G. Monk, M.H. Schmitt, A. Taliercio, M. Velasco, J. Wang, D. Wilbern

Purdue University Northwest, Hammond, Indiana, USA
N. Parashar, A. Pathak, E. Shumka

University of Notre Dame, Notre Dame, Indiana, USA
G. Agarwal, R. Band, R. Bucci, S. Castells, A. Das, A. Datta, A. Ehnis, R. Goldouzian, M. Hildreth, T. Ivanov, C. Jessop, K. Lannon, J. Lawrence,

D. Lutton, J. Mariano, N. Marinelli, P. Mastrapasqua, A. Masud, T. McCauley, C. Mcgrady, C. Moore, Y. Musienko[21], H. Nelson, M. Osherson, A. Piccinelli, R. Ruchti, A. Townsend, Y. Wan, M. Wayne, H. Yockey

Purdue University, West Lafayette, Indiana, USA
S. Chandra, A. Gu, L. Gutay, L. He, M. Huwiler, M. Jones, A.W. Jung, I.G. Karslioglu, D. Kondratyev, J. Li, M. Liu, M. Macedo, G. Negro, N. Neumeister, G. Paspalaki, S. Piperov, N.R. Saha, J.F. Schulte, R. Sharma, F. Wang, A.L. Wesolek, A. Wildridge, W. Xie, Y. Yao, Y. Zhong

The University of Iowa, Iowa City, Iowa, USA
M. Alhusseini, D. Blend, K. Dilsiz[84], O.K. Köseyan, A. Mestvirishvili[56], O. Neogi, H. Ogul[85], Y. Onel, A. Penzo, C. Snyder

The University of Kansas, Lawrence, Kansas, USA
A. Abreu, L.F. Alcerro Alcerro, J. Anguiano, S. Arteaga Escatel, P. Baringer, A. Bean, R. Bhattacharya, M. Chukwuka, Z. Flowers, D. Grove, J. King, G. Krintiras, M. Lazarovits, C. Le Mahieu, J. Marquez, M. Murray, M. Nickel, E. Reynolds, C. Rogan, C. Royon, S. Rudrabhatla, S. Sanders, J.A. Velazquez Corral, G. Wilson

Kansas State University, Manhattan, Kansas, USA
A. Ahmad, B. Allmond, N. Islam, A. Ivanov, K. Kaadze, Y. Maravin, J. Natoli, G.G. Reddy, D. Roy, G. Sorrentino

Johns Hopkins University, Baltimore, Maryland, USA
B. Blumenfeld, J. Davis, A. Gritsan, Z. Huang, L. Kang, P. Maksimovic, N. Pinto, M. Roguljic, S. Sekhar, M.V. Srivastav, M. Swartz

University of Maryland, College Park, Maryland, USA
Z. Alton, D. Baden, A. Belloni, J. Bistany-riebman, S.C. Eno, N.J. Hadley, S. Jabeen, R.G. Kellogg, T. Koeth, B. Kronheim, S. Lascio, J. Lee, P. Major, A. Mignerey, C. Palmer, C. Papageorgakis, M.M. Paranjpe, E. Popova[86], A. Shevelev, M. Wrotny, L. Zhang

Boston University, Boston, Massachusetts, USA
S. Cholak, Z. Demiragli, C. Erice, C. Fangmeier, C. Fernandez Madrazo, J. Fulcher, J. Garcia De Castro, F. Golf, S. Jeon, G. Linney, J. O'Cain, I. Reed, J. Rohlf, D. Sperka, I. Suarez, A. Tsatsos, E. Wurtz, A.G. Zecchinelli

Northeastern University, Boston, Massachusetts, USA
A. Aarif, G. Alverson, E. Barberis, S. Bein, J. Bonilla, B. Bylsma, M. Campana, R. Clark, J. Dervan, Y. Haddad, Y. Han, I. Israr, A. Krishna, M. Lu, N. Manganelli, R. Mccarthy, D.M. Morse, T. Orimoto, L. Skinnari, C.S. Thoreson, E. Tsai, D. Wood

Massachusetts Institute of Technology, Cambridge, Massachusetts, USA
C. Baldenegro Barrera, H. Bossi, S. Bright-Thonney, I.A. Cali, Y.c. Chen, P.c. Chou, M. D'Alfonso, K. Devereaux, J. Eysermans, C. Freer, G. Gomez Ceballos, M. Goncharov, G. Grosso, P. Harris, D. Hoang, G.M. Innocenti, K. Ivanov, G. Kopp, D. Kovalskyi, J. Lang, L. Lavezzo, Y.J. Lee, P. Lugato, C. Mcginn, E. Moreno, A. Novak, M.I. Park, C. Paus, C. Reissel, C. Roland, G. Roland, S. Rothman, T.a. Sheng, G. Stephans, D. Walter, J. Wang, Z. Wang, B. Wyslouch, T. Yang, K. Yoon

Wayne State University, Detroit, Michigan, USA
P.E. Karchin

University of Minnesota, Minneapolis, Minnesota, USA
A. Alpana, B. Crossman, W.J. Jackson, C. Kapsiak, D. Mahon, J. Mans, B. Marzocchi, R. Rusack, O. Sancar, R. Saradhy, N. Strobbe

Bethel University, St. Paul, Minnesota, USA
J.M. Hogan

University of Nebraska-Lincoln, Lincoln, Nebraska, USA
K. Bloom, D.R. Claes, S.V. Dixit, G. Haza, J. Hossain, C. Joo, I. Kravchenko, K.H.M. Kwok, Y. Mehra, J. Morris, A. Rohilla, J.E. Siado, A. Vagnerini, A. Wightman

Rutgers, The State University of New Jersey, Piscataway, New Jersey, USA
B. Chiarito, J.P. Chou, S.V. Clark, S. Donnelly, D. Gadkari, Y. Gershtein, E. Halkiadakis, C. Houghton, D. Jaroslawski, A. Kaur, A. Kobert, I. Laflotte, A. Lath, J. Martins, P. Meltzer, M. Perez Prada, K. Ramdin, B. Rand, J. Reichert, P. Saha, S. Salur, S. Somalwar, R. Stone, S.A. Thayil, S. Thomas, J. Vora

Princeton University, Princeton, New Jersey, USA
H. Bouchamaoui, G. Dezoort, P. Elmer, A. Frankenthal, M. Galli, B. Greenberg, K. Kennedy, Y. Lai, D. Lange, A. Loeliger, D. Marlow, I. Ojalvo, J. Olsen, F. Simpson, D. Stickland, C. Tully, S. Yoon

State University of New York at Buffalo, Buffalo, New York, USA
H. Bandyopadhyay, H.w. Hsia, I. Iashvili, A. Kalogeropoulos, A. Kharchilava, A. Mandal, C. McLean, M. Morris, D. Nguyen, O. Poncet, S. Rappoccio, H. Rejeb Sfar, W. Terrill, A. Williams, D. Yu

Cornell University, Ithaca, New York, USA
J. Alexander, X. Chen, G. De Castro, J. Dickinson, A. Duquette, J. Fan, X. Fan, J. Grassi, P. Kotamnives, K. Krzyzanska, J. Monroy, G. Niendorf, M. Oshiro, J.R. Patterson, A. Ryd, J. Thom, H.A. Weber, B. Weiss, P. Wittich, Y. Wu, R. Zou, L. Zygala

University of Rochester, Rochester, New York, USA
O. Bessidskaia Bylund, A. Bodek, P. de Barbaro, R. Demina, A. Garcia-Bellido, H.S. Hare, O. Hindrichs, N. Parmar, P. Parygin[86], H. Seo, R. Taus, Y.h. Yu

The Ohio State University, Columbus, Ohio, USA
M. Carrigan, R. De Los Santos, L.S. Durkin, C. Hill, M. Joyce, L. Nestor, D.A. Wenzl, B.L. Winer, B. Yates

Carnegie Mellon University, Pittsburgh, Pennsylvania, USA
J. Alison, S. An, M. Cremonesi, V. Dutta, E.Y. Ertorer, T. Ferguson, T.A. Gómez Espinosa, A. Harilal, A. Kallil Tharayil, M. Kanemura, A. Khanal, C. Liu, M. Marchegiani, P. Meiring, S. Murthy, P. Palit, K. Park, M. Paulini, A. Roberts, A. Sanchez, Y. Zhou

University of Puerto Rico, Mayaguez, Puerto Rico, USA
S. Malik, R. Sharma

Brown University, Providence, Rhode Island, USA

G. Barone, G. Benelli, D. Cutts, S. Ellis, S. Gottlieb, L. Gouskos, M. Hadley, L. Hay, U. Heintz, K.W. Ho, R. Jain, T. Kwon, L. Lambrecht, G. Landsberg, K.T. Lau, M. LeBlanc, J. Luo, S. Mondal, J. Roloff, T. Russell, S. Sagir[87], X. Shen, M. Stamenkovic, S. Sunnarborg, J. Tang, N. Venkatasubramanian

University of Tennessee, Knoxville, Tennessee, USA
A. Abdelhamid, D. Ally, A.G. Delannoy, S. Fiorendi, J. Harris, T. Holmes, A.R. Kanuganti, N. Karunarathna, J. Lawless, L. Lee, E. Nibigira, B. Skipworth, S. Spanier, C. Thompson, A. Vendrasco

Vanderbilt University, Nashville, Tennessee, USA
U. Acharya, E. Appelt, Y. Chen, S. Greene, A. Gurrola, W. Johns, R. Kunnawalkam Elayavalli, A. Melo, D. Rathjens, F. Romeo, I. Shvetsov, S. Tuo, J. Velkovska, J. Zhang

Texas A&M University, College Station, Texas, USA
D. Aebi, M. Ahmad, T. Akhter, K. Androsov, A. Basnet, A. Bolshov, O. Bouhali[88], A. Cagnotta, S. Cooperstein, V. D'Amante, R. Eusebi, P. Flanagan, J. Gilmore, Y. Guo, T. Kamon, R. Mueller, G. Pizzati, A. Safonov

Rice University, Houston, Texas, USA
D. Acosta, A. Agrawal, C. Arbour, T. Carnahan, K.M. Ecklund, F.J. Geurts, I. Krommydas, N. Lewis, W. Li, J. Lin, X. Liu, C. Loizides, O. Miguel Colin, B.P. Padley, R. Redjimi, J. Rotter, C. Vico Villalba, M. Wulansatiti, E. Yigitbasi, Y. Zhang

Texas Tech University, Lubbock, Texas, USA
N. Akchurin, J. Damgov, Y. Feng, N. Gogate, W. Jin, S.W. Lee, C. Madrid, S. Magedov, A. Mankel, T. Peltola, I. Volobouev

Baylor University, Waco, Texas, USA
S. Abdullin, A. Brinkerhoff, E. Collins, M.R. Darwish, J. Dittmann, K. Hatakeyama, V. Hegde, J. Hiltbrand, B. McMaster, J. Samudio, S. Sawant, C. Sutantawibul, J. Wilson

University of Virginia, Charlottesville, Virginia, USA
B. Cardwell, H. Chung, B. Cox, J. Hakala, G. Hamilton Ilha Machado, R. Hirosky, M. Jose, A. Ledovskoy, C. Mantilla, R. Menon Raghunandanan, C. Neu, C. Ramón Álvarez, Z. Wu

University of Wisconsin - Madison, Madison, Wisconsin, USA
A. Aravind, S. Banerjee, K. Black, T. Bose, E. Chavez, R. Cruz, S. Dasu, P. Everaerts, C. Galloni, H. He, M. Herndon, A. Herve, C.K. Koraka, S. Lomte, R. Loveless, J. Marquez, A. Mohammadi, S. Mondal, T. Nelson, G. Parida, D. Pinna, A. Savin, V. Sharma, R. Simeon, W.H. Smith, D. Teague, M. Thakore, A. Thete, A. Warden

Authors affiliated with an international laboratory covered by a cooperation agreement with CERN
S. Afanasiev, V. Alexakhin, Y. Andreev, D. Budkouski, R. Chistov, M. Danilov, T. Dimova, I. Gorbunov, A. Kamenev, V. Karjavine, O. Kodolova[89], V. Korenkov, I. Korsakov, A. Kozyrev, A. Lanev, A. Malakhov, V. Matveev, A. Nikitenko[90,89], V. Palichik, V. Perelygin, O. Radchenko, M. Savina, V. Shalaev, S. Shmatov, S. Shulha, Y. Skovpen, K. Slizhevskiy, V. Smirnov, O. Teryaev, A. Toropin,

N. Voytishin, A. Zarubin, I. Zhizhin

Authors affiliated with an institute formerly covered by a cooperation agreement with CERN
L. Dudko, V. Kim[21], V. Murzin, V. Oreshkin, D. Sosnov

[1]Also at Yerevan State University, Yerevan, Armenia
[2]Also at Technische Universität Wien, Vienna, Austria
[3]Also at Ghent University, Ghent, Belgium
[4]Also at FACAMP - Faculdades de Campinas, Sao Paulo, Brazil
[5]Also at Universidade Estadual de Campinas, Campinas, Brazil
[6]Also at Federal University of Rio Grande do Sul, Porto Alegre, Brazil
[7]Also at The University of the State of Amazonas, Manaus, Brazil
[8]Also at University of Chinese Academy of Sciences, Beijing, China
[9]Also at School of Physics, Zhengzhou University, Zhengzhou, China
[10]Now at Henan Normal University, Xinxiang, China
[11]Also at University of Shanghai for Science and Technology, Shanghai, China
[12]Also at The University of Iowa, Iowa City, Iowa, USA
[13]Also at Nanjing Normal University, Nanjing, China
[14]Also at Center for High Energy Physics, Peking University, Beijing, China, Beijing, China
[15]Also at Cairo University, Cairo, Egypt
[16]Also at Zewail City of Science and Technology, Zewail, Egypt
[17]Also at British University in Egypt, Cairo, Egypt
[18]Also at Ain Shams University, Cairo, Egypt
[19]Also at Université de Haute Alsace, Mulhouse, France
[20]Also at Purdue University, West Lafayette, Indiana, USA
[21]Also at an institute formerly covered by a cooperation agreement with CERN
[22]Also at University of Hamburg, Hamburg, Germany
[23]Also at RWTH Aachen University, III. Physikalisches Institut A, Aachen, Germany
[24]Also at Bergische University Wuppertal (BUW), Wuppertal, Germany
[25]Also at Brandenburg University of Technology, Cottbus, Germany
[26]Also at Institute for Advanced Simulation - Jülich Supercomputing Centre, Juelich, Germany
[27]Also at CERN, European Organization for Nuclear Research, Geneva, Switzerland
[28]Also at HUN-REN ATOMKI - Institute of Nuclear Research, Debrecen, Hungary
[29]Now at Universitatea Babes-Bolyai - Facultatea de Fizica, Cluj-Napoca, Romania
[30]Also at MTA-ELTE Lendület CMS Particle and Nuclear Physics Group, Eötvös Loránd University, Budapest, Hungary
[31]Also at HUN-REN Wigner Research Centre for Physics, Budapest, Hungary
[32]Also at Physics Department, Faculty of Science, Assiut University, Assiut, Egypt
[33]Also at The University of Kansas, Lawrence, Kansas, USA
[34]Also at Punjab Agricultural University, Ludhiana, India
[35]Also at University of Hyderabad, Hyderabad, India
[36]Also at University of Visva-Bharati, Santiniketan, India
[37]Also at Institute of Physics, Bhubaneswar, India
[38]Also at Deutsches Elektronen-Synchrotron, Hamburg, Germany
[39]Also at Isfahan University of Technology, Isfahan, Iran
[40]Also at Sharif University of Technology, Tehran, Iran
[41]Also at Department of Physics, University of Science and Technology of Mazandaran, Behshahr, Iran
[42]Also at Department of Physics, Faculty of Science, Arak University, ARAK, Iran
[43]Also at Helwan University, Cairo, Egypt

[44]Also at Kocaeli University, Kocaeli, Türkiye
[45]Also at Centro Siciliano di Fisica Nucleare e di Struttura della Materia, Catania, Italy
[46]Also at James Madison University, Harrisonburg, Virginia, USA
[47]Also at Università degli Studi Guglielmo Marconi, Roma, Italy
[48]Also at Scuola Superiore Meridionale, Università di Napoli 'Federico II', Napoli, Italy
[49]Also at Fermi National Accelerator Laboratory, Batavia, Illinois, USA
[50]Also at Lulea University of Technology, Lulea, Sweden
[51]Also at Consiglio Nazionale delle Ricerche - Istituto Officina dei Materiali, Perugia, Italy
[52]Also at Boston University, Boston, Massachusetts, USA
[53]Also at UPES - University of Petroleum and Energy Studies, Dehradun, India
[54]Also at Institut de Physique des 2 Infinis de Lyon (IP2I), Villeurbanne, France
[55]Also at Department of Applied Physics, Faculty of Science and Technology, Universiti Kebangsaan Malaysia, Bangi, Malaysia
[56]Also at Georgian Technical University, Tbilisi, Georgia
[57]Also at Departamento de Física Instituto Superior Técnico Universidade de Lisboa, Lisbon, Portugal
[58]Also at Trincomalee Campus, Eastern University, Sri Lanka, Nilaveli, Sri Lanka
[59]Also at Saegis Campus, Nugegoda, Sri Lanka
[60]Also at National and Kapodistrian University of Athens, Athens, Greece
[61]Also at Ecole Polytechnique Fédérale Lausanne, Lausanne, Switzerland
[62]Also at Universität Zürich, Zurich, Switzerland
[63]Also at Stefan Meyer Institute for Subatomic Physics (SMI), Vienna, Austria
[64]Also at Near East University, Research Center of Experimental Health Science, Mersin, Türkiye
[65]Also at Konya Technical University, Konya, Türkiye
[66]Also at Izmir Bakircay University Faculty of Engineering and Architecture, Izmir, Türkiye
[67]Also at Adiyaman University, Adiyaman, Türkiye
[68]Also at Istanbul Sabahattin Zaim University, Istanbul, Türkiye
[69]Also at Marmara University, Istanbul, Türkiye
[70]Also at Milli Savunma University, Naval Academy, Istanbul, Türkiye
[71]Also at The Science and Technological research Council of Türkiye, Informatics and Information Security Research Center, Gebze/Kocaeli, Türkiye
[72]Also at Kafkas University, Kars, Türkiye
[73]Now at Istanbul Okan University, Istanbul, Türkiye
[74]Also at Istanbul University - Cerrahpasa, Faculty of Engineering, Istanbul, Türkiye
[75]Also at Istinye University, Istanbul, Türkiye
[76]Also at Mimar Sinan University, Istanbul, Istanbul, Türkiye
[77]Also at Indian Institute of Science (IISC), Bangalore, India
[78]Also at School of Physics and Astronomy, University of Southampton, Southampton, United Kingdom
[79]Also at Monash University, Faculty of Science, Clayton, Australia
[80]Also at Università di Torino, Torino, Italy
[81]Also at California Lutheran University, Thousand Oaks, California, USA
[82]Also at California Institute of Technology, Pasadena, California, USA
[83]Also at United States Naval Academy - Physics Department, Annapolis, Maryland, USA
[84]Also at Bingol University, Bingol, Türkiye
[85]Also at Sinop University, Sinop, Türkiye
[86]Now at another institute formerly covered by a cooperation agreement with CERN
[87]Also at Karamanoğlu Mehmetbey University, Karaman, Türkiye

[88]Also at Hamad Bin Khalifa University (HBKU), Doha, Qatar
[89]Also at Yerevan Physics Institute, Yerevan, Armenia
[90]Also at Imperial College, London, United Kingdom